Original paper

MORB melt metasomatism and deserpentinization in the peridotitic member of Variscan ophiolite: an example of the Braszowice–Brzeźnica serpentinites (SW Poland)

Piotr Marian WOJTULEK[1]*, Jacek PUZIEWICZ[1], Theodoros NTAFLOS[2]

[1] *University of Wrocław, Institute of Geological Sciences, pl. Maksa Borna 9, 50-204 Wrocław, Poland; piotr.wojtulek@uwr.edu.pl*
[2] *University of Vienna, Department of Lithospheric Research, Althanstraße 14, 1090 Vienna, Austria*
[*] *Corresponding author*

The Variscan Braszowice–Brzeźnica Massif (SW Poland) consists of gabbros and serpentinized peridotites with gabbro veins. Antigorite serpentinites form the western part of the Massif, whereas tremolite peridotites, tremolite serpentinites and lizardite–chrysotile serpentinites are found at the contact with granite intrusion in the east. Sparse relics of clinopyroxene, olivine and chromite were studied within the antigorite serpentinites. Clinopyroxene I (Mg# 90.9–93.47, 1.92–3.80 wt. % Al_2O_3) occurs in the neighbourhood of gabbro veins. Its REE patterns are similar to those of clinopyroxene from the mid-ocean ridge gabbros. Clinopyroxene II (Mg# 96.0–97.0) is Al-poor (≤ 0.10 wt. % Al_2O_3). Olivine I (Fo = 90.1–92.3) contains 0.32–0.50 wt. % NiO, whereas olivine II (Fo = 86.0–91.2) is Ni-poor (0.01–0.25 wt. % NiO) and contains micrometric magnetite intergrowths. Chromite I (Cr# 44.9–54.0, Mg# 45.0–52.1, < 0.17 wt. % TiO_2) is associated with olivine I and clinopyroxene I, whereas chromite II (Cr# 43.2–51.4, Mg# = 34.6–47.7, 0.49–0.74 wt. % TiO_2) occurs in serpentinites penetrated by gabbro veins.

The serpentinites of the Braszowice–Brzeźnica Massif were formed supposedly immediately below the paleo-Moho in the ocean-spreading setting. Chemistry of clinopyroxene I from antigorite serpentinites resembles, in terms of major elements and REE, clinopyroxenes that originate due to MORB-like melt percolation through abyssal peridotites. The coexisting olivine I with both chromite I and II supposedly shared a similar origin. Composition of chromite suggests the back-arc setting of the Braszowice–Brzeźnica Massif. Clinopyroxene II and olivine II have major-element compositions indicative of metamorphic origin at expense of serpentine ± magnetite (deserpentinization). The deserpentinization assemblage occurring in serpentinites (antigorite–olivine–clinopyroxene) was formed probably under low-grade metamorphic conditions. The tremolite-bearing rocks record the thermal metamorphism by granite intrusion.

Keywords: Variscan ophiolite, peridotitic member, MORB melt percolation, clinopyroxene, Braszowice–Brzeźnica Massif, Bohemian Massif
Received: 4 December 2016; accepted: 21 June 2017; handling editor: E. Jelínek

1. Introduction

The Rheic Ocean is considered to have formed in the Late Cambrian to Early Ordovician times due to drift of peri-Gondwanan terranes (e.g. Avalonia, Armorica, Ossa-Morena) and to have closed in the Early Devonian (Franke and Dulce 2017). Remnants of the Rheic Ocean in Europe are preserved in the suture running from the Pulo de Lobo Unit of southern Iberia, through Cabo Ortegal Complex in north-western Spain, Lizard Ophiolite in southern Britain, Mid-German Crystalline Rise in Germany to the Bohemian Massif in Central Europe (Murphy et al. 2006; Nance et al. 2010). Mariánské Lázně and the Central-Sudetic ophiolites are two mafic–ultramafic complexes interpreted to be vestiges of the Rheic Ocean in the Bohemian Massif (Jelínek et al. 1997; Nance and Linnemann 2009; Kryza and Pin 2010; Jašarová et al. 2016).

The Variscan Central-Sudetic ophiolites occur in the Sudetes, in the NE part of the Bohemian Massif. They constitute group of gabbroic and serpentinitic outcrops, with subordinate metabasalts (Kryza and Pin 2010). The geochemical affinity of the Central-Sudetic ophiolites has been relatively well studied. The Ślęża Ophiolite, which is the most complete ophiolitic sequence in the region, was considered to having originated in the mid-ocean ridge or back-arc setting (Pin et al. 1988).The peridotite members of the Central-Sudetic ophiolites are heavily serpentinized, nevertheless they contain non-serpentine phases which record information about ocean rift processes and later metamorphism (Wojtulek et al. 2016a, b, and references therein).

In this paper we describe the non-serpentine phases occurring in highly serpentinized ultramafic rocks from the Braszowice–Brzeźnica Massif, a small ophiolite slice belonging to the Central-Sudetic ophiolites. We show that some of these minerals originated due to melt percolation in the uppermost part of the mantle, probably close to the paleo-Moho. We also show that part of the

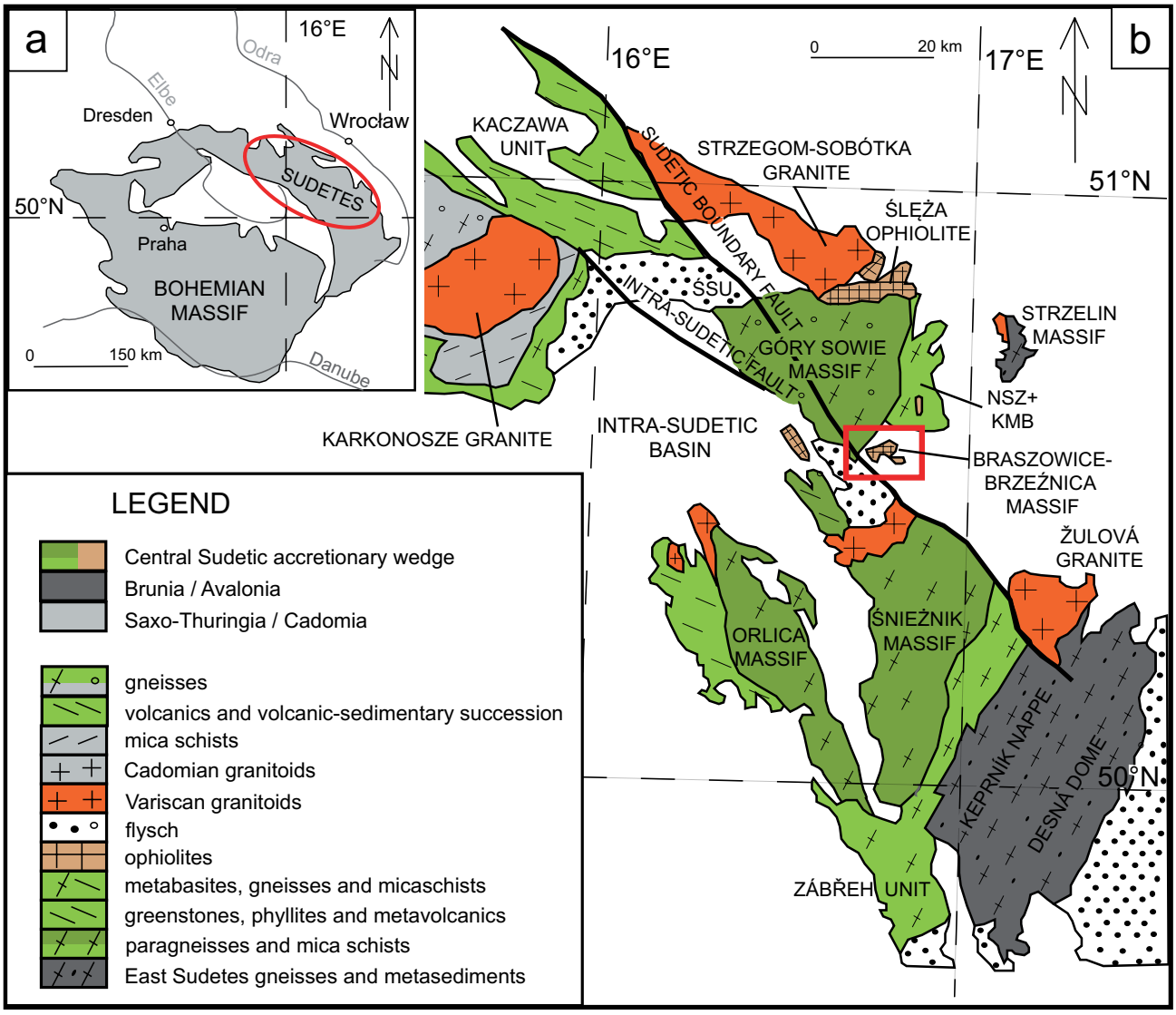

Fig. 1a – Position of Sudetes within the Bohemian Massif in Central Europe. **b** – Location of the Braszowice–Brzeźnica Massif relative to major geological units of Sudetes, modified from Mazur et al. (2015). SSU – Świebodzice sedimentary unit, NSZ – Niemcza shear zone, KMB – Kamieniec metamorphic belt.

non-serpentine phases grew during later metamorphic event, which caused local deserpentinization, and that the Braszowice–Brzeźnica Massif recorded the processes similar to those identified in the peridotitic member of the Ślęża Ophiolite.

2. Geological setting

The Braszowice–Brzeźnica Massif (BBM) is one of the serpentinite–gabbro massifs belonging to the Central-Sudetic ophiolites (Kryza and Pin 2010). It is located in the Central Sudetes Terrane in the NE Bohemian Massif (Fig. 1), which is interpreted as the fragmented accretionary wedge placed between the Saxo-Thuringia and Brunia (Mazur et al. 2015).

The small (~6 km long and ~3 km wide) Braszowice–Brzeźnica Massif is positioned at the southern termination of the Niemcza Shear Zone. Its contacts with surrounding rocks are tectonic except for the eastern part, truncated by a small leucogranite intrusion (Fig. 2). The BBM consists (from N to S) of serpentinites, containing locally chromitite bodies (west of the Grochowiec Hill area), serpentinites with gabbro veins (outcrops on the Mnich Hill) and larger gabbro bodies (small outcrops in the Tarnawa area and a larger body, *c.* 600 m in diameter, in the Braszowice area). The contact between gabbros and serpentinites is exposed in an abandoned quarry on Bukowczyk Hill, where gabbros dip beneath serpentinites along a NE–SW striking boundary (Finckh 1929; Dziedzic 1995). The relationships between gabbros and serpentinites cannot be assessed because of Quaternary

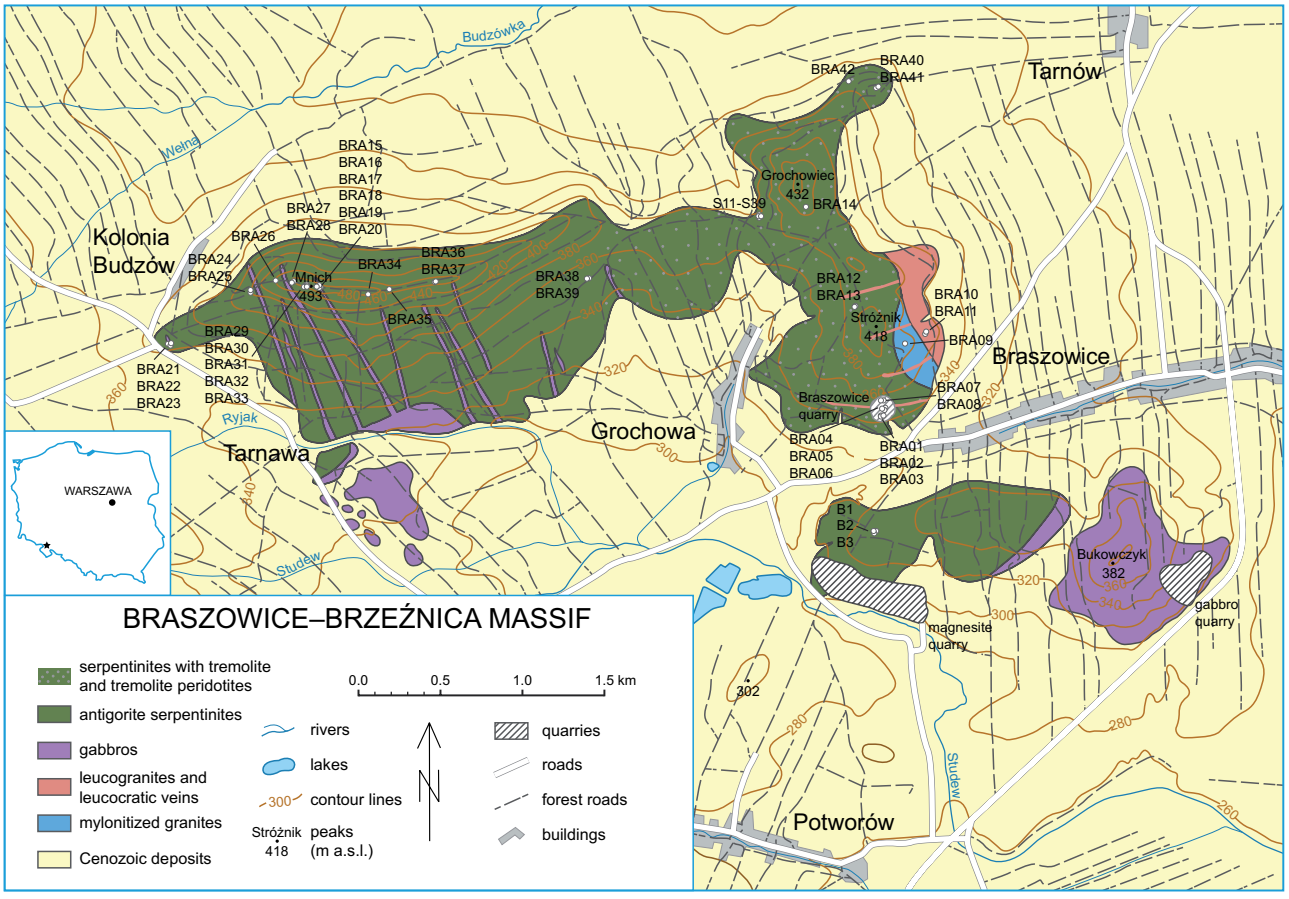

Fig. 2 Geological sketch map of the Braszowice–Brzeźnica Massif (compiled by Michał Dajek, based on maps of Gaździk 1957 and Oberc et al. 1996). The serpentine types after Gunia (1992).

sediments cover. The drillings between Tarnawa and Bukowczyk revealed serpentinites with gabbro inliers under the Quaternary cover (Dziedzic 1995). Gabbros from drillings and those from Tarnawa are medium- or fine-grained, whereas gabbros on Bukowczyk Hill and in Braszowice are mainly coarse-grained (Dziedzic 1995).

The tremolite peridotites and serpentinites with inliers of lizardite–chrysotile serpentinites form the eastern part of the massif, whereas the western part consists of antigorite serpentinites with gabbro veins (Gunia 1992). Serpentinite–magnesite–dolomite breccias, magnesite veins and bodies, rodingite and pyroxenite veins or irregular bodies occur mostly in the western BBM (Gunia 1992). Serpentinites of the eastern part of the massif are cut by aplite veins, and chromitite bodies were described in the centre (Delura 2012; Wojtulek et al. 2016a). Gabbros occur in the southern and eastern parts of the BBM. They are isotropic or laminated and are moderately deformed (Dziedzic 1989; Delura 2012).

The age of the serpentinites and gabbros is assumed to be analogous to that of the matching rock types of the Ślęża Ophiolite (Dziedzic and Dziedzic 2000). Few zircon grains from a Ślęża metagabbro were investigated by Oliver et al. (1993). These authors used the conventional U–Pb method on abraded zircons. The calculated age of 420 + 20/– 2 Ma was related to the magmatic crystallization of the gabbro (Oliver et al. 1993). More recently, magmatic crystallization of zircon grains from metagabbros and metabasalts in the Ślęża Ophiolite was dated at 400 ± 10 Ma and 403 ± 6 Ma by Kryza and Pin (2010), by the SHRIMP method. Zircons from the contact zone between rodingite and serpentinite gave a U–Pb age of 400 + 4/– 3 Ma, interpreted as timing the early serpentinization (Dubińska et al. 2004).

3. Sampling and analytical methods

This paper is based on 42 samples (Fig. 2) collected from outcrops located mostly at peaks of hills and abandoned quarries. We used 150 μm thick sections for microscopic and chemical investigations.

3.1. Mineral chemistry

The major-element composition of minerals from 20 samples has been analysed by Cameca SX-100 electron microprobe at Department of Lithospheric Research,

Tab. 1 Whole-rock major (wt. %) and trace (ppm) element analyses of rocks from the BBM

Sample	Detection limit	Eastern part of the BBM					Western part of the BBM				
		Braszowice quarry				Grochowiec	Mnich				
		BRA01	BRA04	BRA07	BRA12	BRA14	BRA16	BRA17	BRA18	BRA19	BRA20
Rock type		Tremolite peridotite	Tremolite peridotite	Tremolite peridotite	Tremolite serpentinite	Pseudomorphic serpentinite	Metagabbro	Metagabbro	Antigorite serpentinite	Antigorite serpentinite	Dunite vein
SiO_2	0.01	43.42	49.60	47.80	41.22	40.19	42.51	44.53	40.38	39.13	38.71
TiO_2	0.01	0.31	0.04	0.08	<0.02	0.01	0.13	0.14	<0.02	<0.02	0.01
Al_2O_3	0.01	5.92	1.68	4.45	0.64	0.56	17.27	14.57	1.10	0.75	0.24
Cr_2O_3	0.02	0.83	0.40	0.30	0.24	0.47	0.27	0.36	0.42	0.39	0.05
$Fe_2O_3^*$	0.04	7.30	5.76	4.79	8.74	10.05	3.93	3.58	7.92	8.04	15.18
MnO	0.01	0.05	0.07	0.07	0.13	0.13	0.08	0.10	0.07	0.12	0.18
MgO	0.01	27.37	28.25	27.44	41.59	41.28	12.77	12.75	38.79	40.91	39.09
CaO	0.01	7.06	8.04	7.85	0.32	0.48	18.38	20.16	0.23	0.48	0.07
Na_2O	0.01	0.04	0.05	0.05	0.02	<0.02	0.11	0.18	<0.02	<0.01	<0.02
K_2O	0.01	0.01	0.02	0.02	<0.02	<0.02	0.02	<0.02	<0.02	<0.01	<0.02
P_2O_5	0.01	0.24	0.03	0.01	0.02	0.02	<0.01	0.02	<0.02	<0.01	0.02
LOI	–	7.30	5.80	6.90	6.70	6.50	4.20	3.30	10.70	8.90	6.20
Sum	–	99.85	99.74	99.76	99.62	99.69	99.67	99.69	99.61	98.72	99.75
Sc	1.0	21	13	9	8	7	21	26	11	9	6
Ba	1.0	<1	<1	10	2	<1	30	17	2	<1	2
Be	1.0	<1	<1	<1	<1	<1	<1	<1	3	<1	<1
Co	0.2	45.3	56.9	57.4	120.2	117.1	37.4	27.9	93.9	105.8	131.9
Cs	0.1	0.2	0.3	0.6	<0.1	<0.1	0.1	<0.1	<0.1	<0.1	<0.1
Ga	0.5	3.9	1.1	3.8	<0.05	<0.05	8.8	4.0	0.7	0.9	<0.05
Hf	0.1	1.2	<0.1	0.9	0.1	<0.1	0.2	<0.1	<0.1	<0.1	<0.1
Nb	0.1	0.9	0.4	1.4	<0.1	0.8	0.3	<0.1	<0.1	<0.1	<0.1
Rb	0.1	0.3	0.2	0.8	0.4	0.2	0.4	0.3	1.3	<0.1	<0.1
Sn	1.0	1.0	<1	<1	<1	<1	<1	<1	<1	<1	<1
Sr	0.5	43.1	34.9	66.0	3.5	2.3	388.4	1850.1	19.3	2.3	3.6
Ta	0.1	0.1	<0.1	<0.1	<0.1	<0.1	<0.1	<0.1	<0.1	<0.1	<0.1
Th	0.2	2.6	<0.02	3.8	<0.02	<0.02	<0.2	<0.02	<0.02	<0.2	<0.02
U	0.1	0.5	0.7	1.5	<0.1	<0.1	<0.1	<0.1	<0.1	<0.1	<0.1
V	8.0	120	68	62	22	47	68	107	47	38	19
W	0.5	<0.05	2.0	0.6	0.6	0.8	<0.5	<0.05	<0.05	20.1	<0.05
Zr	0.1	39.8	1.7	28.6	1.1	1.4	5.2	5.9	0.7	0.3	1.1
Y	0.1	5.0	2.2	3.2	0.2	0.1	2.3	3.8	0.3	0.1	0.4
La	0.1	5.2	0.5	1.5	0.5	0.4	0.5	1.1	0.7	0.2	0.7
Ce	0.1	10.5	0.6	3.5	0.5	0.2	0.7	1.6	0.4	<0.1	0.4
Pr	0.02	1.60	0.05	0.55	<0.02	<0.02	0.11	0.18	<0.02	<0.02	<0.02
Nd	0.03	7.00	<0.03	2.60	<0.03	<0.03	0.70	1.00	<0.03	<0.03	<0.03
Sm	0.05	1.42	<0.05	0.92	<0.05	<0.05	0.23	0.23	<0.05	<0.05	<0.05
Eu	0.02	0.12	0.04	0.18	<0.02	<0.02	0.14	0.44	<0.02	<0.02	<0.02
Gd	0.05	1.16	0.32	0.88	<0.05	<0.05	0.38	0.55	<0.05	<0.05	<0.05
Tb	0.01	0.19	0.07	0.14	<0.02	<0.02	0.07	0.12	<0.02	<0.01	0.02
Dy	0.05	1.31	0.41	0.79	<0.05	0.06	0.51	0.63	0.07	<0.05	<0.05
Ho	0.02	0.22	0.04	0.10	<0.02	<0.02	0.09	0.17	<0.02	<0.02	<0.02
Er	0.1	0.61	0.21	0.35	0.09	<0.01	0.25	0.36	0.03	<0.03	0.09
Tm	0.01	0.08	0.03	0.05	<0.01	<0.01	0.05	0.06	<0.01	<0.01	<0.01
Yb	0.05	0.62	0.24	0.24	<0.05	<0.05	0.26	0.34	<0.05	<0.05	<0.05
Lu	0.01	0.10	0.04	0.04	0.01	0.01	0.03	0.04	<0.01	<0.01	0.01
Mo	0.1	<0.01	<0.01	<0.01	0.10	0.20	0.10	0.10	<0.01	<0.10	<0.01
Cu	0.1	17.8	29.2	50.2	3.5	11.1	2.7	8.0	10.8	3.5	202.8
Pb	0.1	1.1	0.7	2.8	0.3	0.2	1.3	0.4	1.2	0.2	1.2
Zn	1.0	12	12	11	29	34	15	20	15	45	45
Ni	0.1	787	1236	1001	2487	2556	246.9	477	2075	1997.1	1870
As	0.5	1.2	1.1	1.4	2.0	1.3	0.6	<0.05	5.4	1.3	3.8

*total Fe as Fe_2O_3

University of Vienna, Austria under standard conditions (acceleration voltage 15 kV, sample current 15 nA, counting times 10 or 20 s, natural silicates and synthetic oxides as standards) and using the PAP correction procedure (Pouchou and Pichoir 1984). The structural formulae of minerals were recalculated on the basis of 4 O for olivine, 23 O for tremolite, 6 O for clinopyroxene, 3 cations for spinel and 2 cations for ilmenite. Chromium number, Cr#, is defined as atomic 100 × Cr/(Cr + Al) and magnesium number, Mg#, as atomic 100 × Mg/(Mg + Fe) in mineral formulae. Mineral abbreviations used are after Kretz (1983).

The trace element-contents in clinopyroxene were determined by laser-ablation ICP-MS technique in a serpentinite (BRA19) and a gabbro (BRA17). The former was analysed at the Kraków Research Centre, Institute of Geological Sciences, Polish Academy of Sciences. For details of analytical procedure see Wojtulek et al. (2016b). The latter was analysed at the Institute of Geology of the Czech Academy of Science in Prague using an Element 2 ICP-MS coupled with an UP-213 213-nm NdYAG laser ablation system. The repetition rate of 20 Hz and the output energy of 12 J/cm^2 were applied. Circular, beam ablation spots were 60 μm in diameter. Sample runs were bracketed by measurements of NIST 612 glass (Jochum et al. 2011). The electron-microprobe determined Ca content was used as an internal standard. Data were processed using the Glitter software (van Achterbergh et al. 2001).

3.2. Whole-rock geochemistry

Eight samples were crushed with a jaw crusher and pulverized in an agate mill at Bureau Veritas Analytical Laboratory in Vancouver, Canada (*http://acmelab.com*). Then, bulk-rock chemical compositions (major-, minor- and trace-elements) of the samples were analysed by inductively coupled plasma mass spectrometry (ICP-MS), using analytical procedures with codes LF100 and LF300. Detection limits for each measured element are given in Tab. 1.

4. Petrography and mineral chemistry

4.1. Eastern part of the Braszowice–Brzeźnica Massif

Eastern part of the BBM consists of tremolite peridotites, tremolite serpentinites and amphibole–chlorite rocks (Fig. 2). Tremolite peridotites were described as "dunites" with more than 90 vol. % of olivine by Gunia (1992). They are relatively weakly serpentinized (~10–20 vol. % of serpentine) and are cut by serpentine veinlets. The peridotites contain numerous magnesite veins in the vicinity of the granite intrusion. Non-serpentine mineral grains are isolated from each other by serpentine or chlorite. Tremolite content varies usually between ~5 and 10 vol. %.

Olivine in both *tremolite peridotites and serpentinites* occurs as dismembered, up to 200 μm grains cut by tremolite and serpentine, enclosing magnetite inclusions (Fig. 3a). Olivine has mainly constant chemical composition ($Fo_{90.5–91.1}$, 0.35–0.45 wt. % NiO, 0.15–0.17 wt. % MnO – Fig. 4, Tab. 2), however, some analyses reveal variation in NiO (up to 0.70 or down to 0.11 wt. %) and MnO (up to 0.21 or down to 0.11 wt. %) contents, but without correlation to a specific occurrence. Serpentine replaces olivine and forms a network of veins. Tremolite (Tab. 3) forms needle-like, elongated grains that cut ol-

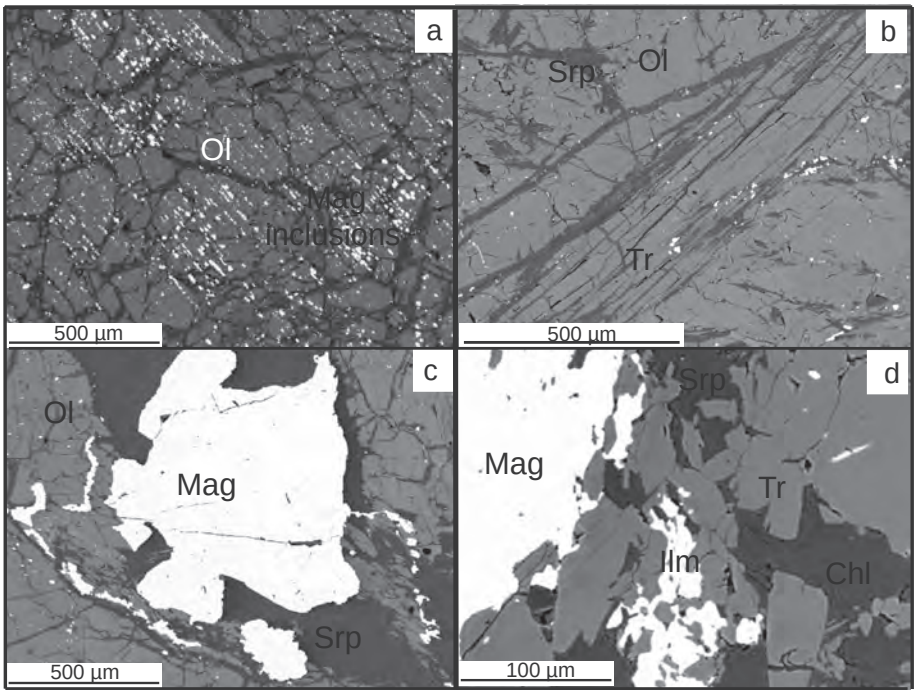

Fig. 3 Back-scattered electron images of rocks occurring in the eastern part of the Braszowice–Brzeźnica Massif. **a** – Olivine with parallel magnetite inclusions (BRA14). **b** – Serpentinized olivine–tremolite aggregate (BRA13). **c** – Cr-rich magnetite and olivine in lizardite/chrysotile serpentinite from Grochowiec Hill (BRA04). **d** – Magnetite–tremolite–chlorite–ilmenite aggregate from amphibole–chlorite rock (BRA01).

Tab. 2 Representative chemical analyses (wt. %) and structural formulae (O = 4) of olivine from the BBM serpentinites

Location	Eastern part					Western part						
Olivine type	Ol I	Ol I	Ol I	Ol II	Ol II	Ol I	Ol I	Ol I	Ol II	Ol II	Ol from dunite vein	Ol from dunite vein
Sample	BRA01	BRA14	BRA40	BRA14	BRA40	BRA18	BRA21	BRA34	BRA18	BRA34	BRA20	BRA20
SiO_2	40.89	41.02	41.21	41.15	41.13	41.36	41.65	40.95	41.29	40.47	39.87	39.88
TiO_2	0.01	0.00	0.00	0.00	0.00	0.02	0.00	0.02	0.00	0.00	0.00	0.01
Al_2O_3	0.05	0.01	0.00	0.00	0.00	0.00	0.02	0.01	0.01	0.00	0.00	0.00
Cr_2O_3	0.00	0.00	0.03	0.05	0.00	0.05	0.04	0.09	0.07	0.08	0.01	0.00
FeO*	9.42	8.81	8.41	8.80	8.69	7.90	7.06	8.48	9.65	11.92	14.96	15.74
MnO	0.18	0.16	0.16	0.16	0.15	0.27	0.26	0.31	0.57	0.97	0.26	0.25
NiO	0.38	0.39	0.44	0.29	0.27	0.44	0.45	0.44	0.15	0.18	0.22	0.23
MgO	49.00	49.63	49.94	49.49	50.06	50.16	51.36	49.99	48.67	46.25	43.93	44.14
CaO	0.01	0.02	0.01	0.02	0.01	0.01	0.02	0.02	0.02	0.04	0.13	0.14
Total	99.96	100.03	100.19	99.96	100.32	100.21	100.85	100.31	100.45	99.93	99.41	100.41
Si	1.00	1.00	1.00	1.00	1.00	1.00	1.00	1.00	1.01	1.01	1.01	1.00
Ti	0.00	0.00	0.00	0.00	0.00	0.00	0.00	0.00	0.00	0.00	0.00	0.00
Al	0.00	0.00	0.00	0.00	0.00	0.00	0.00	0.00	0.00	0.00	0.00	0.00
Cr	0.00	0.00	0.00	0.00	0.00	0.00	0.00	0.00	0.00	0.00	0.00	0.00
Fe	0.19	0.18	0.17	0.18	0.18	0.16	0.14	0.17	0.20	0.25	0.32	0.33
Mn	0.00	0.00	0.00	0.00	0.00	0.01	0.01	0.01	0.01	0.02	0.01	0.01
Ni	0.01	0.01	0.01	0.01	0.01	0.01	0.01	0.01	0.00	0.00	0.00	0.01
Mg	1.79	1.81	1.81	1.80	1.81	1.82	1.84	1.81	1.77	1.71	1.65	1.65
Ca	0.00	0.00	0.00	0.00	0.00	0.00	0.00	0.00	0.00	0.00	0.00	0.00
%Fo**	90.09	90.80	91.21	90.77	90.98	91.63	92.60	91.02	89.46	86.47	83.72	83.11

*total Fe as FeO
**[100 × Mg/(Mg + Fe)] atoms per formula unit

Tab. 3 Representative chemical analyses (wt. %) and structural formulae (O = 23) of tremolite from the Eastern part of the BBM

Location	Eastern part				
Rock type	Tremolite peridotite	Tremolite peridotite	Chlorite–tremolite rock	Pseudomorphic serpentinite	Tremolite peridotite
Sample	BRA01	BRA04	BRA13	BRA14	BRA40
SiO_2	58.62	58.80	58.58	58.73	58.75
TiO_2	0.12	0.01	0.04	0.00	0.00
Al_2O_3	0.28	0.23	0.06	0.07	0.03
FeO*	1.80	1.56	1.31	1.40	1.62
MnO	0.04	0.07	0.04	0.04	0.06
MgO	23.80	23.93	23.77	23.82	23.88
CaO	13.46	13.14	13.61	13.81	13.57
Na_2O	0.05	0.13	0.00	0.00	0.01
K_2O	0.03	0.01	0.00	0.00	0.03
Total	98.20	97.88	97.41	97.87	97.95
Si	7.96	7.99	8.00	7.99	7.99
Ti	0.01	0.00	0.00	0.00	0.00
Al	0.04	0.04	0.01	0.01	0.00
Fe	0.20	0.18	0.15	0.16	0.18
Mn	0.00	0.01	0.00	0.00	0.01
Mg	4.82	4.85	4.84	4.83	4.84
Ca	1.96	1.91	1.99	2.01	1.98
Na	0.01	0.03	0.00	0.00	0.00
K	0.01	0.00	0.00	0.00	0.01
Total	15.02	15.01	14.99	15.01	15.01
Mg#**	95.9	96.5	97.0	96.8	96.3

*total Fe as FeO
**[100 × Mg/(Mg + Fe)] atoms per formula unit

ivine (Fig. 3b) or fills veins. It becomes a major rock-forming mineral in some samples (e.g. BRA07). Magnetite occurs as rectangular inclusions in olivine up to 20 μm across. Magnetite grains are often parallel-arranged and are similar to magnetite occurring in bastite pseudomorphs. Locally, magnetite forms rounded or amoeboid grains up to 500 μm (Fig. 3c, Tab. 4). Minute inclusions have ilmenite composition, whereas larger grains contain up to 30.40 wt. % Cr_2O_3.

The *chlorite–tremolite rocks* occur together with tremolite peridotites in the Braszowice abandoned quarry, closest to the leucogranite intrusion, but observations of field relationships are impossible because of high degree of weathering. Thin sections show that they consist of chlorite, tremolite and accessory ilmenite. Tremolite has composition similar to that of the same phase in tremolite peridotites (Tab. 3). Chlorite fills interstices between tremolite grains (Fig. 3d).

It is almost purely magnesian (Mg# = 0.93–0.95). Ilmenite (Tab. 4) occurs in samples coming from the vicinity to granite intrusion. It forms intergrowths with tremolite (Fig. 3d).

4.2. Western part of the Braszowice–Brzeźnica Massif

This region consists of antigorite serpentinites with locally occurring non-serpentine phases and metagabbro veins (Gunia 1992, Fig. 5).

Antigorite serpentinites display mainly non-pseudomorphic texture (Fig. 6a); pseudomorphic bastite or mesh textures are rare (Fig. 6b). Serpentine constitutes more than 80 vol. % of the rock, forming groundmass dominated by rosette-shaped aggregates. The non-serpentine phases occur in the serpentine groundmass in two assemblages: (1) clinopyroxene I – chromite I – olivine I – chromite II and (2) clinopyroxene II – olivine II. Serpentine fills fractures in clinopyroxene parallel to cleavage or forms network within olivine.

Olivine I and II differ by Mg and Ni contents: olivine I ($Fo_{90.1–92.3}$) contains 0.32–0.50 wt. % NiO, whereas olivine II ($Fo_{86.0–91.2}$) has only 0.01–0.25 wt. % NiO (Fig. 4, Tab. 2). Olivine II commonly contains magnetite inclusions which have various sizes (2–25 μm) and are locally parallel-arranged and are overgrown by serpentine (Fig. 6c). Both kinds of olivine occur in aggregates: olivine I forms well-crystallized, dismembered, magnetite-free grains included in olivine II – serpentine – magnetite groundmass (Fig. 6c). Olivine II and serpentine fills also fissures between dismembered grains of olivine I.

Clinopyroxene is diopside or augite (Fig. 7a, Tab. 5). Clinopyroxene I has Mg# 90.9–93.47 and contains 1.92–3.80 wt. % Al_2O_3 and 0.75–1.33 wt. % Cr_2O_3 (Fig. 7b). Clinopyroxene I occurs in serpentinites cut by gabbro veins. Its grains are strongly dismembered and have well defined cleavage. It forms two textural varieties:

(a) Coarse (up to 0.7 mm in size), elongated, discrete grains occurring in serpentine groundmass (Fig. 6d). They have Mg# 91.0–93.1, are Ti- and Na-rich (0.70–0.80 wt. % TiO_2 and 0.33–0.48 wt. % Na_2O) and contain 3.23–3.80 wt. % Al_2O_3 and 1.09–1.33 wt. % Cr_2O_3. The rare earth elements are enriched relative to primitive mantle (Fig. 8, Tab. 6). The REE patterns show LREE depletion relative to HREE and shallow negative Eu anomaly. Zirconium content varies between 28 and 36 ppm.

(b) Coarse, up to 0.5 mm, anhedral grains, often elongated, occurring interstitially in aggregates with olivine I and chromite I (Fig. 6e). These clinopyroxenes have Mg# 90.9–93.47 and contain 1.92–3.07 wt. % Al_2O_3 and

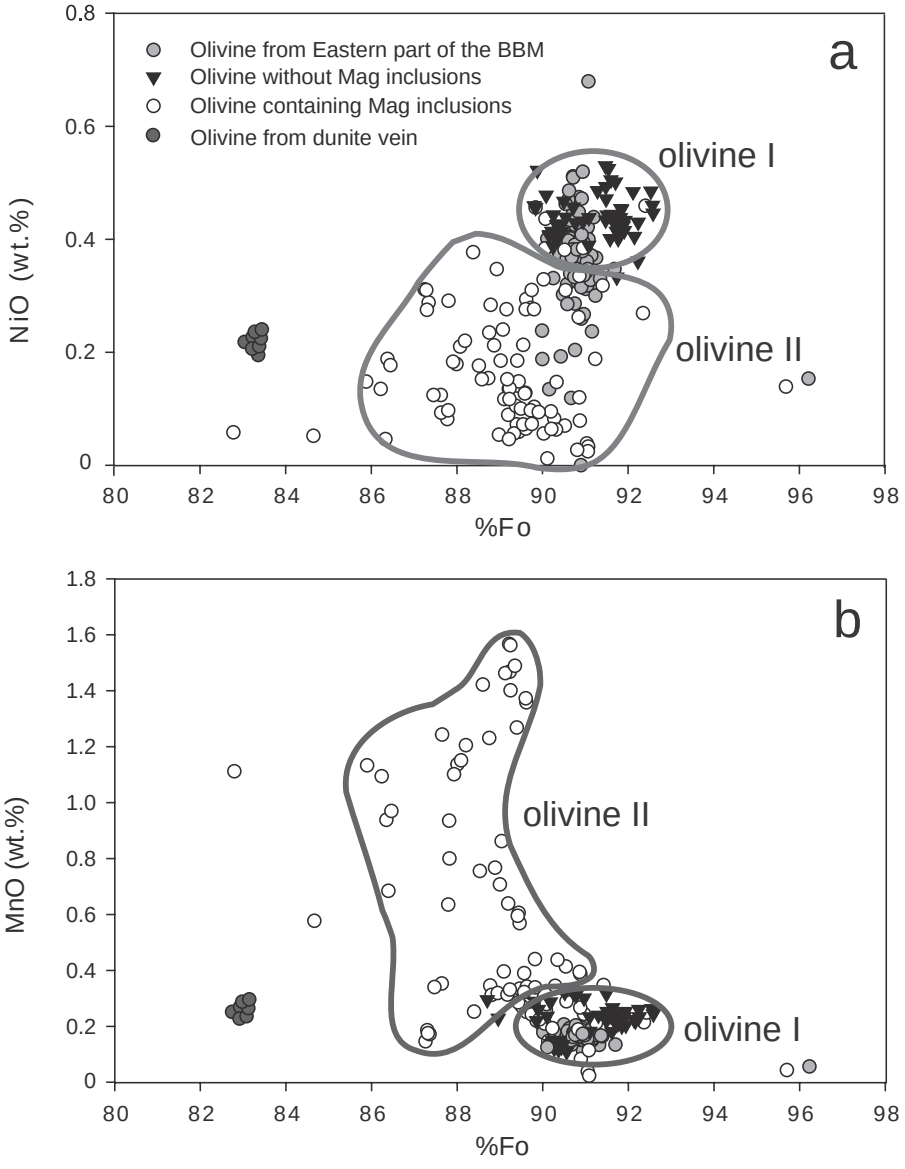

Fig. 4 Relationships between forsterite (mol. %) and chemical compositions of olivine from the Braszowice–Brzeźnica Massif (wt. %): NiO (**a**) and MnO (**b**).

Tab. 4 Representative chemical analyses (wt. %) and structural formulae of spinel (sum of cations = 3) and ilmenite (sum of cations = 2) from the BBM serpentinites

Location	Eastern part of the BBM					Western part of the BBM											
Mineral*	1	1	2	2	3	2	2	3	3	4	4	4	4	5	5	5	5
Sample	BRA01	BRA01	BRA04	BRA14	BRA04	BRA18	BRA34	BRA18	BRA34	BRA19	BRA19	BRA35	BRA35	BRA34	BRA34	BRA39	BRA39
SiO_2	0.06	0.05	0.00	0.01	0.04	0.01	0.00	0.24	0.00	0.00	0.00	0.00	0.00	0.00	0.02	0.00	0.00
TiO_2	51.19	51.04	0.64	0.40	0.07	0.16	0.60	0.07	0.24	0.63	0.63	0.72	0.74	0.14	0.15	0.02	0.00
Al_2O_3	0.00	0.00	0.33	0.57	0.00	0.00	1.41	0.02	0.09	26.21	26.41	27.16	27.09	26.50	26.05	25.39	25.56
Cr_2O_3	0.25	0.24	30.40	27.17	0.00	16.71	31.60	0.45	2.30	38.18	38.23	31.19	31.15	39.13	38.52	40.64	41.18
FeO[a]	44.32	43.96	59.96	62.19	89.86	70.40	55.34	88.93	87.79	23.12	23.10	29.25	29.82	21.06	22.86	20.49	19.91
MnO	2.45	2.34	0.68	0.42	0.04	0.90	2.35	0.09	0.13	0.49	0.52	0.43	0.34	0.23	0.53	0.46	0.47
NiO	0.03	0.05	0.44	0.57	0.27	0.63	0.48	0.64	0.70	0.09	0.10	0.18	0.17	0.11	0.13	0.03	0.09
MgO	0.74	0.77	2.38	2.71	0.18	1.69	1.97	0.94	0.66	10.26	9.99	9.17	8.84	11.84	10.39	10.61	10.97
CaO	0.08	0.12	0.00	0.04	0.00	0.01	0.33	0.00	0.00	0.01	0.02	0.63	0.50	0.24	0.36	1.07	0.90
Total	99.14	98.57	99.12	98.57	94.83	94.08	90.46	90.51	94.08	91.38	91.91	98.99	99.00	98.73	98.65	99.25	99.01
Ti	0.97	0.98	0.02	0.01	0.00	0.00	0.02	0.00	0.01	0.01	0.01	0.02	0.02	0.00	0.00	0.00	0.00
Al	0.00	0.00	0.01	0.03	0.00	0.00	0.06	0.00	0.00	0.96	0.97	0.99	1.00	0.96	0.95	0.93	0.93
Cr	0.01	0.01	0.91	0.81	0.00	0.52	0.95	0.01	0.07	0.94	0.94	0.77	0.77	0.95	0.94	1.00	1.01
Fe^{+3}[b]	0.06	0.05	1.04	1.19	2.00	1.49	0.98	2.01	1.91	0.13	0.07	0.31	0.23	0.12	0.12	0.14	0.12
Fe^{+2}	0.88	0.88	0.85	0.78	0.98	0.83	0.78	0.89	0.94	0.47	0.53	0.45	0.54	0.42	0.47	0.39	0.39
Mn	0.05	0.05	0.02	0.01	0.00	0.03	0.08	0.00	0.00	0.01	0.01	0.01	0.01	0.01	0.01	0.01	0.01
Ni	0.00	0.00	0.01	0.02	0.01	0.02	0.01	0.02	0.02	0.00	0.00	0.00	0.00	0.00	0.00	0.00	0.00
Mg	0.03	0.03	0.13	0.15	0.01	0.10	0.11	0.05	0.04	0.47	0.46	0.42	0.41	0.54	0.48	0.49	0.51
Cr#	–	–	–	–	–	–	–	–	–	49.42	49.27	43.51	43.55	49.76	49.80	51.78	51.94

*1 – ilmenite, 2 – coarse, amoeboid magnetite grains, 3 – minute magnetite inclusions, 4 – chromite I, 5 – chromite II

[a] Total Fe as FeO

[b] Calculated by charge balance

0.75–1.20 wt. % Cr_2O_3 (Fig. 7b). Their TiO_2 and Na_2O contents are very low (< 0.1 wt. % – Fig. 7c).

Relationships between Al_2O_3 and Cr_2O_3 in clinopyroxene I reveal a continuous trend in which both oxides correlate positively (Fig. 7b). Contents of TiO_2 and Na_2O are variable on a sample scale, although clinopyroxene I (a) from aggregates with olivine I is generally Ti- and Na-poor (Fig. 7c).

Clinopyroxene II has high Mg# (96.0–97.0) and is Al- and Cr-poor (≤ 0.10 wt. % Al_2O_3 and ≤ 0.27 wt. % Cr_2O_3). It occurs as (1) lamellae within serpentine and olivine I and II, (2) as minute elongated grains, up to 50 µm long, occurring in aggregates with olivine II and (3) as large (up to 3 mm) grains

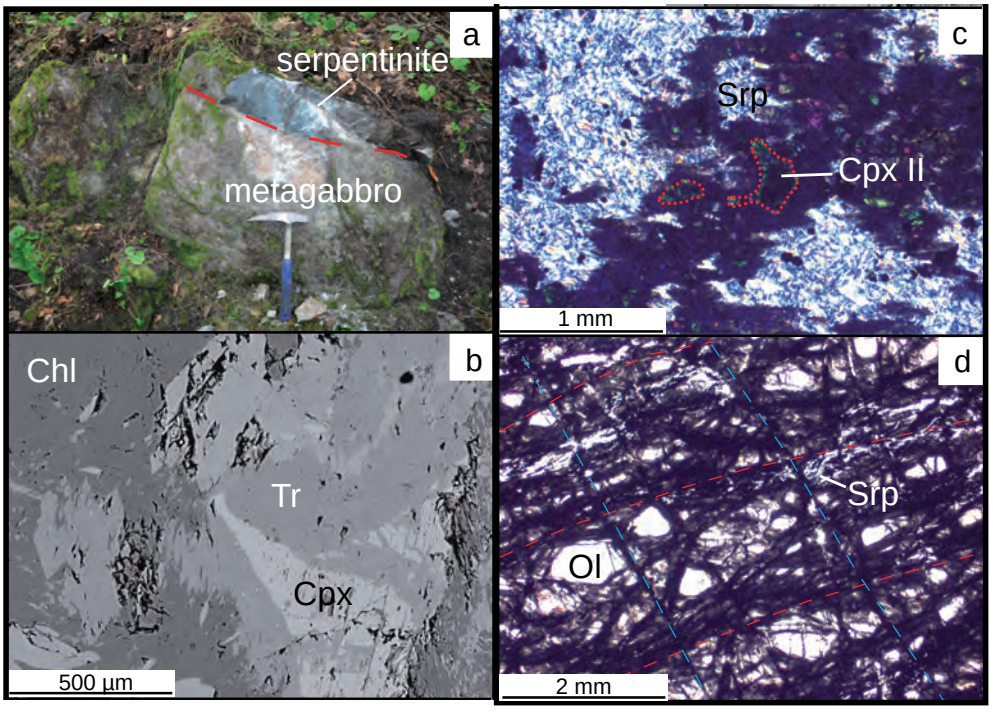

Fig. 5 Photographs of rocks occurring in the western part of the Braszowice–Brzeźnica Massif. **a** – Contact between serpentinite and metagabbroic vein. **b** – Chlorite–tremolite–clinopyroxene assemblage in metagabbro. Tremolite replaces clinopyroxene, BSE image (BRA25). **c** – Anhedral clinopyroxene aggregate in the serpentine groundmass of serpentinite, plane-polarised light (PPL) image (BRA19). **d** – Mylonitized dunite, PPL (BRA18).

with cleavage and parallel-arranged minute magnetite inclusions, locally displaying mesh texture (Fig. 6f). Clinopyroxene II does not occur together with clinopyroxene I, and thus interpretation of their mutual relations is not possible. Trace elements were not measured in clinopyroxene II due to insufficient sizes of its grains.

Chromite from antigorite serpentinites forms zoned grains up to 2 mm in size. Two types were distinguished (Fig. 9, Tab. 4). Chromite I (Cr# 44.9–54.0, Mg# 45.0–52.1) contains up to 0.17 wt. % TiO_2 and occurs in aggregates with olivine I and clinopyroxene I (Fig. 6g). Chromite II (Cr# 43.2–51.4, Mg# = 34.6–7.7) is richer in TiO_2 (0.49–0.74 wt. %) and occurs in serpentinites penetrated by gabbro veins. Rims of the zoned chromite I – chromite II grains consist of ferritchromite (Fig. 6h).

Gabbro and dunite veins occur in serpentinites at the Mnich Hill (Fig. 5, Tab. 1). Gabbro veins are from *c.* 10 cm to more than 1 m wide. We found also loose gabbro blocks ~1.2 × 1.4 × 1.6 m in size displaying weak layering. Layers of variable clinopyroxene contents are from 2 to 7 cm thick. Diopside from gabbro veins has similar major-element composition to coarse clinopyroxene Ia from antigorite serpentinites (Mg# 88.0–90.5, Al_2O_3 3.17–3.65 wt. %, Cr_2O_3 0.74–1.09 wt. %, TiO_2 0.40–0.79 wt. %, Na_2O 0.31–0.51 wt. % – Fig. 7; Tab. 5). Shape of the REE patterns is similar to that in clinopyroxene I from serpentinites but without negative Eu anomaly (Fig. 8, Tab. 6).

The dunite veins, up to 5 cm thick, cut serpentinites together with metagabbro veins. Olivine grains in the dunite veins are highly fractured, arranged parallel to the main fracture direction (Fig. 5d). Olivine from these veins is relatively Mg-poor ($Fo_{83.4–83.7}$) and contains 0.21–0.23 wt. % NiO and 0.22–0.39 wt. % MnO (Fig. 4, Tab. 2).

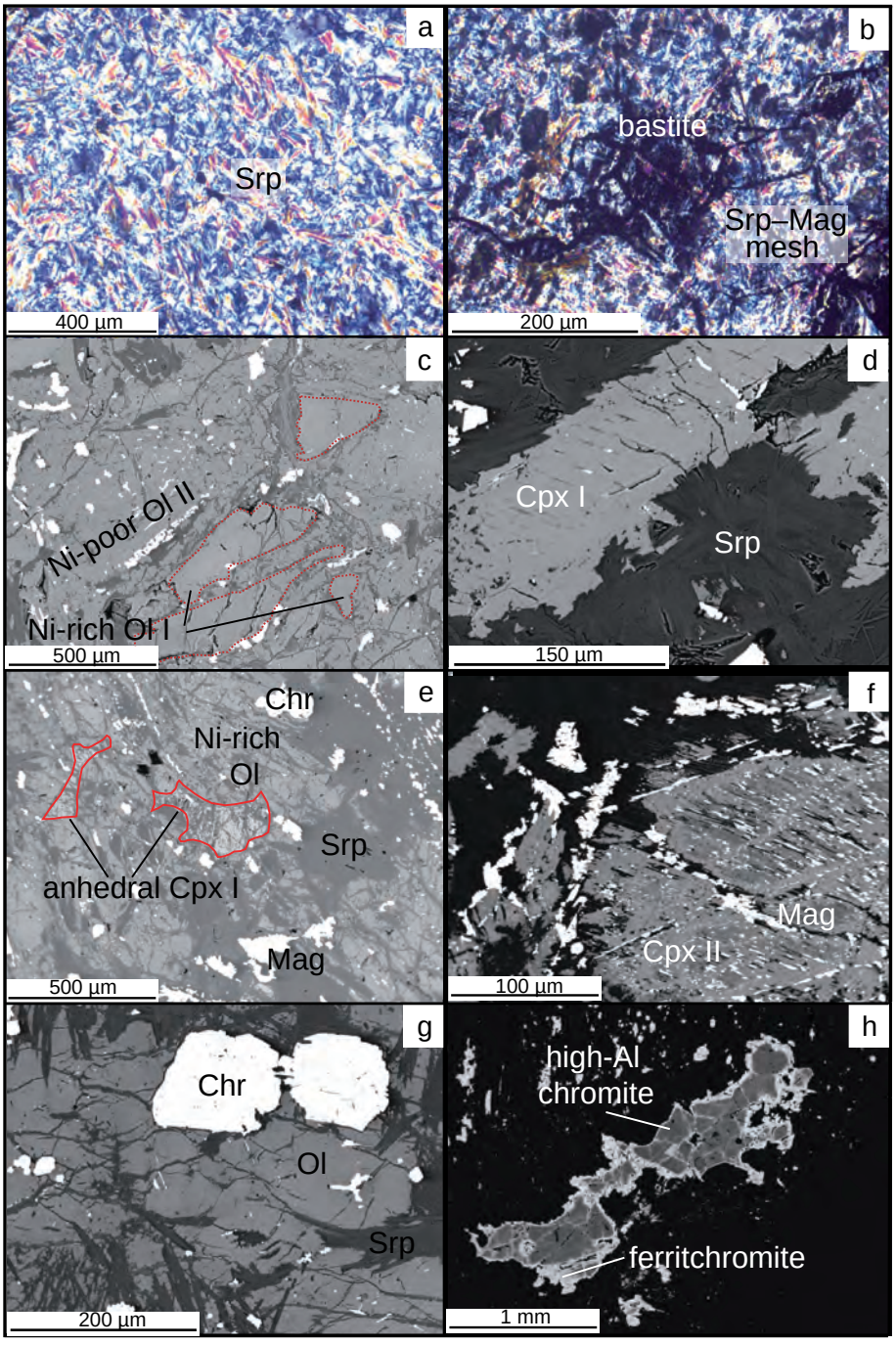

Fig. 6 Photomicrographs of serpentinites occurring in the western part of the Braszowice–Brzeźnica Massif. **a** – Non-pseudomorphic serpentinite, PPL (BRA18). **b** – Relict of pseudomorphic bastite and mesh texture, PPL (BRA22). **c** – Aggregate consisting of olivine I (magnetite-free) and olivine II (magnetite-bearing), BSE image (BRA21). **d** – Large clinopyroxene II grains, BSE image (BRA19). **e** – Aggregates consisting of olivine I and anhedral clinopyroxene I, BSE image (BRA22). **f** – Large clinopyroxene II grain displaying mesh texture with parallel magnetite inclusions, BSE image (BRA29). **g** – Rounded chromite I–olivine I aggregate, BSE image (BRA18). **h** – Amoeboid chromite II, BSE image (BRA34).

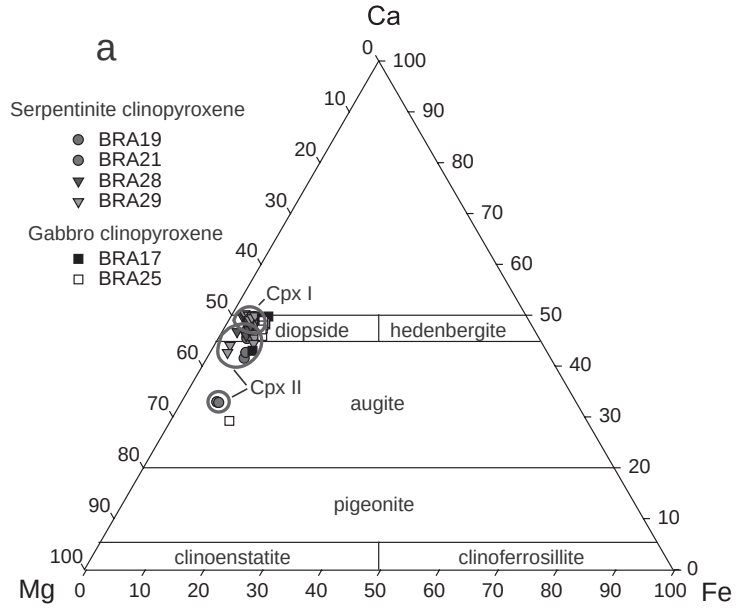

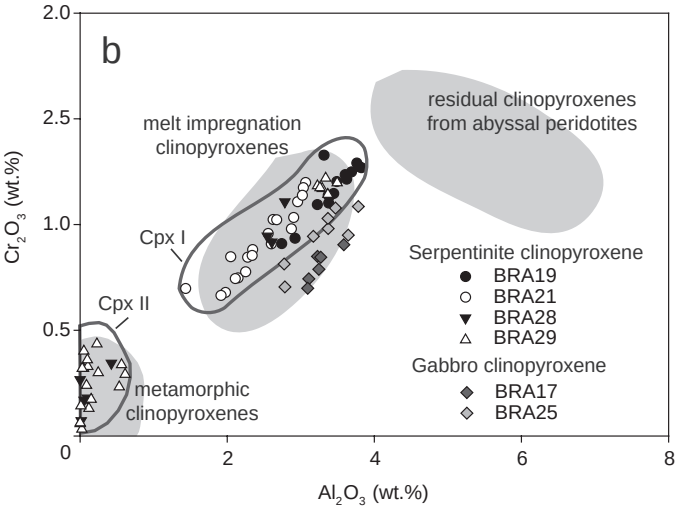

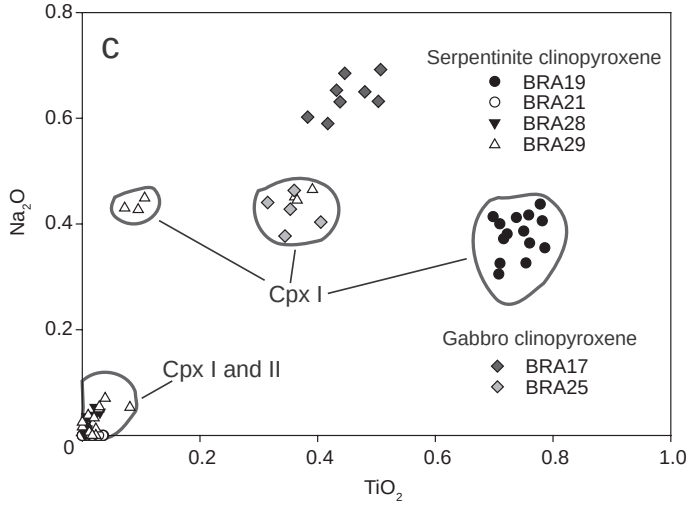

5. Whole-rock geochemistry

Ultramafic rocks from both parts of the Braszowice–Brzeźnica Massif have distinct whole-rock compositions. In the Eastern part, tremolite peridotites are richer in CaO (7.06–8.04 wt. %) and Al_2O_3 (1.68–5.92 wt. %) than tremolite and pseudomorphic serpentinites (0.32–0.48 wt.% CaO; 0.56–0.64 wt.% Al_2O_3 – Tab. 1). The former have also elevated concentrations of both fluid-mobile (Cs, Rb, Th and Pb) and fluid immobile (REE) trace elements, whereas tremolite and pseudomorphic serpentinites show contents of most trace elements below detection limits of the applied method.

In the Western part of the BBM, antigorite serpentinites and dunite are poor in CaO (0.07–0.48 wt. %), Al_2O_3 (0.24–1.10 wt. %) and trace elements (Tab. 1). They are only slightly enriched in Nb, Rb and Pb relative to Primitive mantle (McDonough and Sun 1995). Other trace elements are below their respective detection limits, except for Ba (2 ppm), Sr (2.3–19.3 ppm), Cu (3.5–10.8 ppm), Zn (15–45 ppm), Pb (0.2–1.2 ppm) and As (1.3–5.4 ppm).

Metagabbros are generally depleted in trace elements; their Primitive mantle normalized patterns show only positive anomalies in Ba, Pb and Sr (Fig. 10).

6. Discussion

6.1. Eastern part of the Braszowice–Brzeźnica Massif

Tremolite-bearing serpentinite in the eastern part resembles serpentinites from other parts of the BBM because it contains pseudomorphic bastite, mesh and non-pseudomorphic serpentine and magnetite-bearing olivine but modal and chemical compositions are different. Olivine including magnetite occurs also in tremolite peridotites, thus we suggest that both tremolite-bearing serpentinite and tremolite peridotite developed from tremolite-free rocks occurring

Fig. 7 Composition of clinopyroxene from serpentinites and gabbros of the western Braszowice–Brzeźnica Massif. **a** – Classification diagram after Morimoto et al (1988). **b** – Cr_2O_3 versus Al_2O_3 (wt. %) diagram. Fields representing typical compositions of residual, melt impregnation (Seyler et al. 2007) and metamorphic (Nozaka and Shibata 1995) clinopyroxenes are shown for comparison. **c** – Na_2O versus TiO_2 (wt. %) diagram.

Tab. 5 Representative chemical analyses (wt. %) and structural formulae (O = 6) of clinopyroxene from the Western part of the BBM serpentinites and metagabbros

Cpx generation*	I								II		from metagabbro	
Sample	BRA19	BRA19	BRA29	BRA29	BRA21	BRA21	BRA28	BRA28	BRA29	BRA29	BRA17	BRA25
SiO_2	52.18	51.90	52.62	52.65	53.77	53.66	53.11	53.39	55.05	55.36	52.59	52.04
TiO_2	0.79	0.72	0.10	0.07	0.01	0.00	0.03	0.02	0.01	0.01	0.43	0.63
Al_2O_3	3.45	3.69	3.29	3.34	2.15	2.35	2.78	2.55	0.15	0.02	3.09	3.17
Cr_2O_3	1.15	1.25	1.17	1.22	0.75	0.88	1.11	0.95	0.17	0.03	0.70	0.94
FeO*	2.61	2.53	3.03	2.91	2.34	2.36	2.66	2.56	1.02	1.02	3.21	3.70
MnO	0.13	0.11	0.11	0.10	0.11	0.10	0.08	0.09	0.07	0.08	0.11	0.14
NiO	0.04	0.04	0.02	0.04	0.07	0.07	0.07	0.09	0.01	0.04	0.04	0.02
MgO	16.04	15.85	16.10	15.91	17.49	17.21	17.81	17.48	17.96	17.98	15.93	15.77
CaO	23.49	23.72	23.18	23.63	24.07	24.07	22.95	23.58	25.76	26.09	24.18	23.30
Na_2O	0.35	0.38	0.43	0.43	0.00	0.00	0.04	0.04	0.04	0.00	0.35	0.44
K_2O	0.00	0.02	0.00	0.00	0.00	0.00	0.00	0.00	0.00	0.00	0.01	0.00
Total	100.22	100.21	100.05	100.30	100.87	100.83	100.65	100.74	100.23	100.64	100.64	100.14
Si	1.90	1.89	1.92	1.92	1.94	1.94	1.92	1.93	1.99	1.99	1.91	1.905
Ti	0.02	0.02	0.00	0.00	0.00	0.00	0.00	0.00	0.00	0.00	0.01	0.017
Al	0.15	0.16	0.14	0.14	0.09	0.10	0.12	0.11	0.01	0.00	0.13	0.137
Cr	0.03	0.04	0.03	0.04	0.02	0.03	0.03	0.03	0.00	0.00	0.02	0.027
Fe	0.08	0.08	0.09	0.09	0.07	0.07	0.08	0.08	0.03	0.03	0.10	0.113
Mn	0.00	0.00	0.00	0.00	0.00	0.00	0.00	0.00	0.00	0.00	0.00	0.004
Ni	0.00	0.00	0.00	0.00	0.00	0.00	0.00	0.00	0.00	0.00	0.00	0.001
Mg	0.87	0.86	0.88	0.86	0.94	0.93	0.96	0.94	0.97	0.97	0.87	0.861
Ca	0.92	0.93	0.91	0.92	0.93	0.93	0.89	0.91	1.00	1.01	0.94	0.914
Na	0.03	0.03	0.03	0.03	0.00	0.00	0.00	0.00	0.00	0.00	0.02	0.031
K	0.00	0.00	0.00	0.00	0.00	0.00	0.00	0.00	0.00	0.00	0.00	0.00
Mg#	91.6	91.5	90.7	90.5	93.1	93.0	92.3	92.2	97.0	96.9	90.0	88.4

* Total Fe as FeO

in the western and central parts of the BBM. Occurrence of tremolite as an interstitial phase or in veins suggests its late crystallization.

Since the small leucogranite outcrop is located to the east of the Braszowice–Brzeźnica Massif (Fig. 2), we assume that it induced contact metamorphism of the serpentinites, resulting in increasing amphibole and decreasing serpentine contents towards the contact. It affected the whole-rock Ca contents in ultramafic rocks: unaltered serpentinites from Mnich Hill contain less CaO (0.07–0.23 wt. %) than tremolite-bearing serpentinites from Grochowiec and Stróżnik hills (0.32–0.48 wt. %) and tremolite peridotites (7.06–8.04 wt. %). Tremolite peridotites are also enriched in Al_2O_3 (1.68–5.92 wt. %) and in numerous trace elements (Cs, Hf, Ga, V, Zr, Y, Nb, Ta, U, Th, W and REE), whereas tremolite serpentinites have trace-

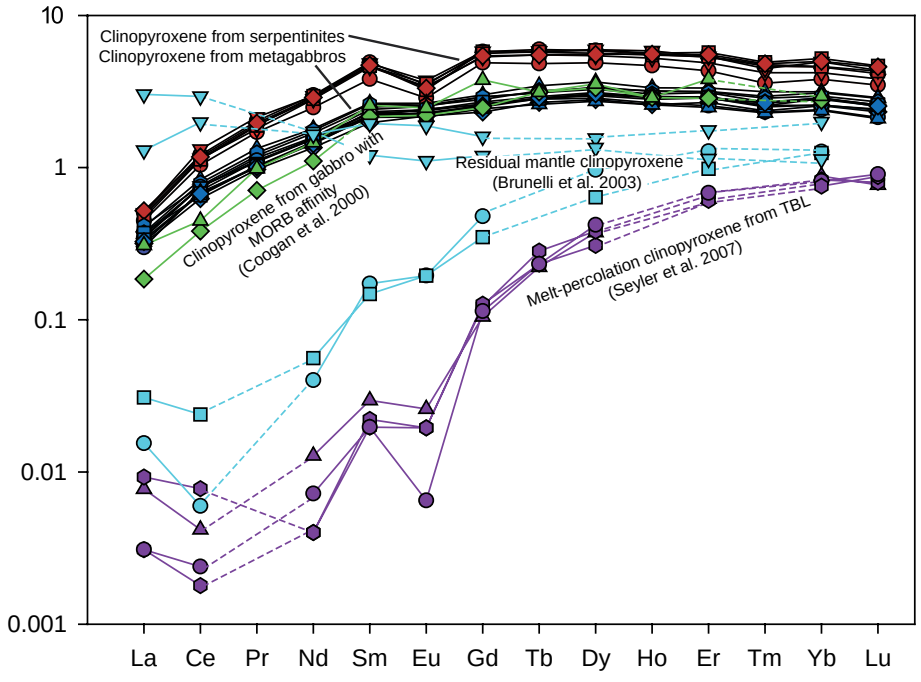

Fig. 8 Primitive mantle-normalised (McDonough and Sun 1995) REE patterns of clinopyroxene I from serpentinite (red) and clinopyroxene from metagabbro (dark blue) of the BBM compared to residual mantle clinopyroxene (Brunelli et al. 2003), melt percolation clinopyroxene (Seyler et al. 2007) and clinopyroxene from gabbro with MORB affinity (Coogan et al. 2000).

Tab. 6 Representative chemical analyses (ppm) of REE in clinopyroxenes from the western part of the BBM serpentinites and metagabbros

Cpx generation	I				from metagabbro			
Sample	BRA19	BRA19	BRA19	BRA19	BRA17	BRA17	BRA17	BRA17
La	0.328	0.318	0.301	0.338	0.264	0.238	0.268	0.227
Ce	2.028	1.918	1.887	1.970	1.398	1.239	1.272	1.262
Pr	0.514	0.456	0.478	0.498	0.339	0.294	0.304	0.277
Nd	3.740	3.520	3.690	3.610	2.250	1.981	2.110	1.919
Sm	1.993	1.863	1.888	1.911	1.075	0.977	1.015	0.924
Eu	0.539	0.524	0.548	0.512	0.407	0.389	0.395	0.364
Gd	3.140	2.900	3.060	2.950	1.787	1.662	1.725	1.531
Tb	0.591	0.545	0.571	0.544	0.341	0.307	0.317	0.282
Dy	3.960	3.660	3.980	3.740	2.459	2.281	2.229	2.027
Ho	0.828	0.780	0.843	0.830	0.498	0.472	0.476	0.432
Er	2.333	2.135	2.501	2.416	1.460	1.386	1.377	1.251
Tm	0.316	0.286	0.335	0.327	0.214	0.200	0.194	0.174
Yb	2.020	1.851	2.302	2.202	1.387	1.366	1.301	1.130
Lu	0.280	0.2585	0.315	0.310	0.194	0.192	0.182	0.163

element compositions similar to antigorite serpentinites from the western BBM. The probably small leucogranite intrusion is surrounded by a narrow (*c.* 750 m) contact aureole. Larger granite intrusions produce much broader contact aureoles in serpentinites, as seen e.g. in the Ohsa-yama serpentinite body (Japan), where it is up to 2 km wide (Nozaka and Shibata 1995). The Ohsa-yama serpentinite changes from unaltered serpentinites (zone I), through serpentinites with olivine, tremolite and talc (zone II) to serpentinites with olivine, orthopyroxene, tremolite and green spinel (zone III; Nozaka and Shibata 1995). The Malenco serpentinite (Italian Alps), which was affected by the Bergell tonalite, is altered from serpentinite consisting of antigorite, diopside, olivine and magnetite into serpentinites with abundant olivine, tremolite, talc, anthophyllite and enstatite (Trommsdorff and Evans 1972 and 1977). In the BBM, Ohsa-yama and Malenco aureoles olivine and tremolite are abundant, whereas diopside vanishes in the altered zone, because of olivine and tremolite formation at expense of antigorite and diopside (Trommsdorff and Evans 1972; Trommsdorff and Connolly 1996). In the BBM, as opposite to Ohsa-yama and Malenco, no orthopyroxene occurs in the vicinity of the leucogranite intrusion which implies that the conditions of pyroxene-hornfels facies were not reached (Frost 1975).

6.2. Western part of the Braszowice–Brzeźnica Massif

Although the whole-rock Al_2O_3/SiO_2 and MgO/SiO_2 ratios (Fig. 11) from the western part of the BBM suggest harzburgite protolith, these rocks do not contain any remnants of orthopyroxene. Non-serpentine minerals that survived serpentinization – olivine, clinopyroxene and chromian spinel – indicate rather wehrlite as a primary lithology. However, remnants of non-serpentine phases are scarce (< 10 vol. %) and thus not representative of the modal composition of the pre-serpentine protolith.

An important message which is hidden in the bulk-rock chemical composition is that the serpentinites are extremely depleted in trace elements, especially those preferentially soluble in hydrous fluids that migrate through serpentinites in various settings (As, Sb, Pb, Sr, Rb, Cs, Li, Ba and U, for details see Deschamps et al. 2013). This composition is related to the texture of the BBM serpentinites, which consist of non-pseudomorphic serpentine groundmass enclosing pseudomorphic domains (serpentine bastite or mesh textures) and non-serpentine minerals (olivine, clinopyroxene and chromian spinel). Textural relationships show that antigorite serpentinization,

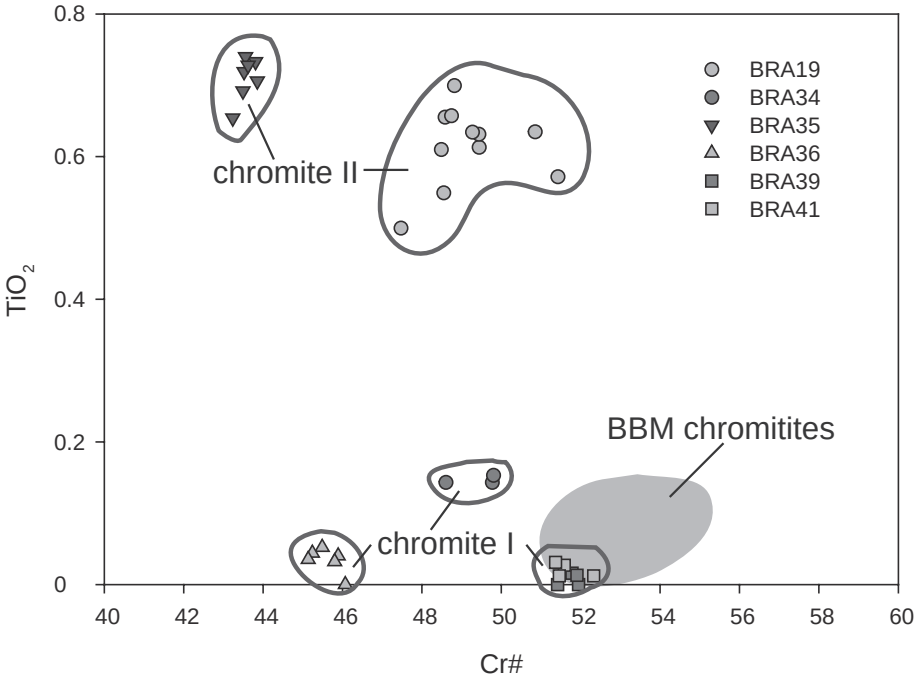

Fig. 9 Relationships between Cr# and TiO_2 (wt. %) in chromite from the Braszowice–Brzeźnica Massif.

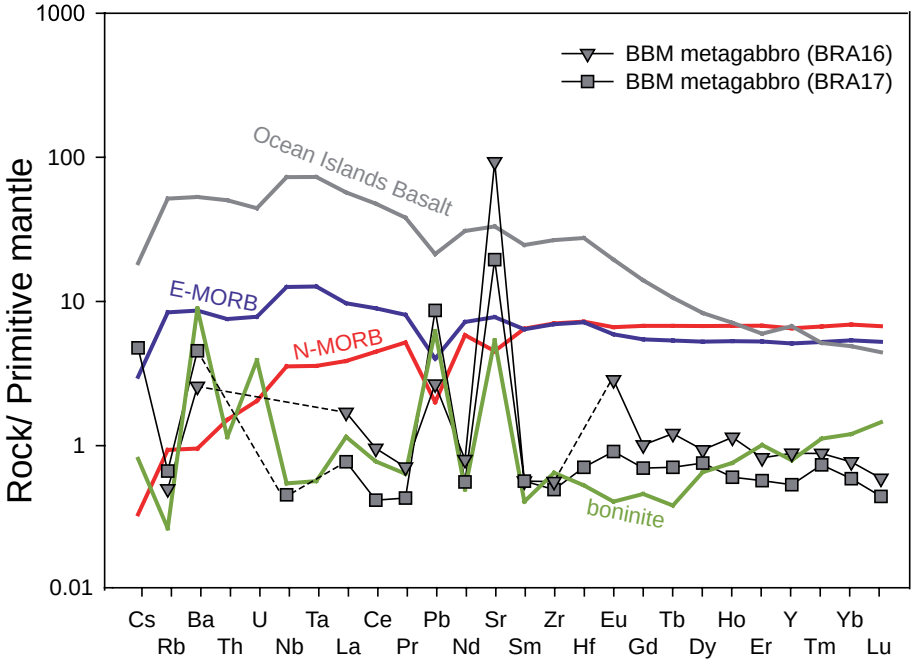

Fig. 10 Primitive mantle-normalised (McDonough and Sun 1995) whole-rock trace-element patterns of gabbros from the western part of the Braszowice–Brzeźnica Massif. Patterns of N-MORB, E-MORB, Ocean Islands Basalt (Sun and McDonough 1989) and boninite (Bédard 1999) are shown for comparison.

producing non-pseudomorphic rocks, overprinted the pseudomorphic serpentinites (Wicks and Whittaker 1977). Serpentinites that underwent antigorite recrystallization are typically depleted in fluid-mobile elements because during the lizardite–antigorite transition the low-T serpentine is replaced by a high-T one containing less water in its structure. This results in partial liberation of water, which may leach fluid-mobile elements from the minerals (Kodolanyi and Pettke 2011; Deschamps et al. 2013). This process takes place at temperatures above 400 °C (Evans 2010). Similar depletion is also typical of metagabbro veins within the BBM serpentinites (Fig. 10) suggesting that they were depleted in trace elements during the same metamorphic event like the serpentinites.

The style of serpentinization in the BBM is similar to that in other serpentinite massifs belonging to the Central-Sudetic Ophiolites: the Gogołów–Jordanów and Szklary. They also recorded at least two steps of alteration: pseudomorphic and non-pseudomorphic ones (Dubińska and Gunia 1997; Wojtulek et al. 2016b).

The non-serpentine mineral assemblages consist of minerals with different modes of occurrence and chemical compositions, having formed supposedly in various events. Clinopyroxene I grains have homogenous chemical composition (Mg#, Al_2O_3 and Cr_2O_3 contents), except for Na_2O and TiO_2, which are higher in isolated grains than in those coexisting with olivine I and chromite I. The Al_2O_3 content of clinopyroxene I is lower than in clinopyroxene from porphyroclastic residual abyssal peridotites, e.g. Bouvet Triple Junction in South Atlantic (3.55–4.87 wt. % Al_2O_3: Brunelli et al. 2003) or Southwest Indian Ridge (4.21–6.35 wt. % Al_2O_3: Seyler et al. 2003). Thus, clinopyroxene I is probably not a phase coming from residual mantle. Its mode of occurrence and composition resemble clinopyroxenes that originated due to melt percolation, e.g. at the Mid-Atlantic Ridge (ODP Hole 1274 A) which contain 1.9–3.62 wt. % Al_2O_3 and 0.50–1.58 wt. % Cr_2O_3 (Seyler et al. 2007) and also form elongated, interstitial grains between olivine grains or at olivine triple-junctions (Suhr et al. 2008). This clinopyroxene was interpreted as a product of interaction between basaltic melt and harzburgite host, replacing orthopyroxene along grain boundaries and/or filling interstices (Suhr et al. 2008). Another phase typically crystallizing during basaltic melt percolation is plagioclase, described both from oceanic (Mariana Trough – Ohara et al. 2002) and ophiolitic peridotites (Oman Ophiolite – Koga et al. 2001). This mineral has not been observed in the BBM serpentinites nor in harzburgites from the ODP Hole 1274 A (Seyler et al 2007). Lack of "impregnation" plagioclase in the BBM serpentinites is supposedly due to undersaturation of metasomatising melt in this phase.

The REE pattern of clinopyroxene I has a well-defined negative Eu anomaly suggesting depletion of parental melt in plagioclase component. In contrast, clinopyroxene from gabbro veins cutting serpentinite lacks Eu anomaly (Fig. 8). This suggests that clinopyroxene from gabbros crystallized before plagioclase, whereas the clinopyroxene I crystallized from, or equilibrated with, melt which fractionated plagioclase. The REE pattern of the clinopyroxene I is similar to that of clinopyroxenes from mid-ocean ridge gabbros (see Coogan et al. 2000) (Fig. 8).

The major-element compositions of clinopyroxene I and clinopyroxene from gabbro differ in terms of Cr_2O_3, Al_2O_3, Na_2O and TiO_2 contents. Moreover, clinopyroxene I itself does not form a uniform group because of variable

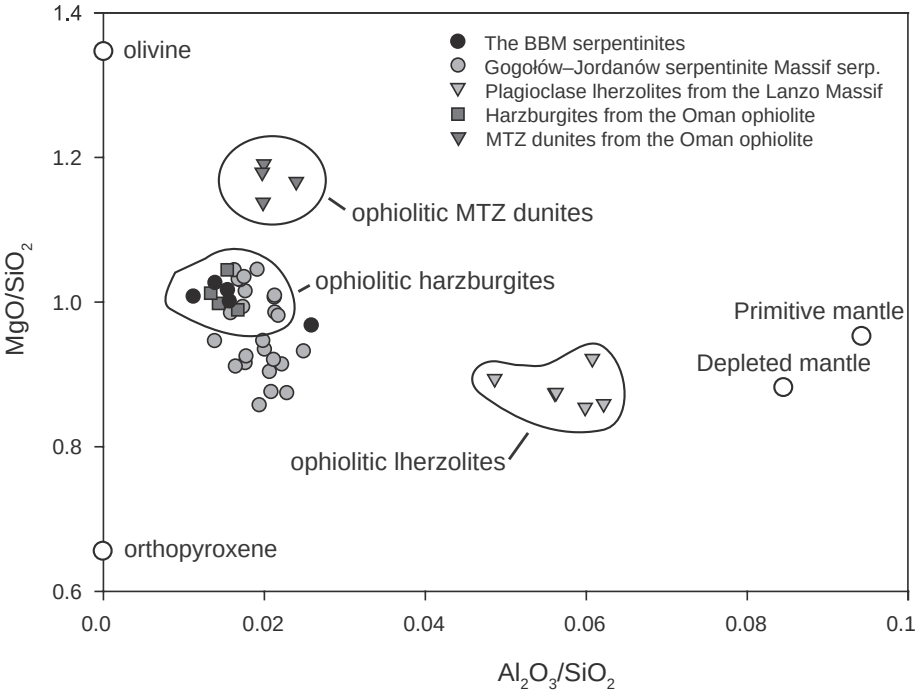

Fig. 11 The MgO/SiO_2 vs. Al_2O_3/SiO_2 diagram for the serpentinized peridotites of the Braszowice–Brzeźnica Massif. Points representing ophiolitic dunites, harzburgites (Godard et al. 2000), ophiolitic lherzolites (Bodinier 1988) and serpentinites from the Gogołów–Jordanów serpentinite Massif (Wojtulek et al. 2016b) are added for comparison.

TiO_2 and Na_2O contents (Fig. 7c). Chemical variation of clinopyroxene I possibly resulted from either varying initial composition of the basaltic melt percolating the peridotite or its chromatographic fractionation.

The Cr# of chromite I and the Mg# of coexisting olivine I fall in the olivine–spinel mantle array (OSMA) defined by Arai (1994) (Fig. 12a). Chemical compositions of chromite I and olivine I are similar both to abyssal peridotites and supra-subduction zone peridotites. Irregular, amoeboid shapes of chromite I indicate its formation in interstices between other mineral grains, a feature typical of grains crystallizing from transient melt. Intermediate Cr# suggests that this melt was MORB-like, but not as depleted as boninites which crystallize high-Cr# spinels (Tamura and Arai 2006; Morishita et al. 2011) . Intermediate Mg# of chromite I (Fig. 12b) suggests back-arc basalt as a potential melt from which chromites crystallized. Back-arc basin as potential setting for melt percolation of the BBM peridotites was also suggested from chromitites (Wojtulek 2016a).

Olivine I has similar Mg# and Ni contents as residual olivine from oceanic abyssal peridotites (Brunelli et al. 2003, 2006) and as olivine that originated due to melt percolation together with clinopyroxene (Seyler et al. 2007). Textural features of grains cannot serve as criterion distinguishing between residual and melt-percolation olivine, because the grains were strongly altered and fragmented during serpentinization. Relationships of olivine I, olivine II and clinopyroxene II lamellae suggest that olivine II and clinopyroxene III crystallized later.

Low Al_2O_3 and Cr_2O_3 contents and elevated Mg# in clinopyroxene II and low NiO with high MnO in olivine II are typical of metamorphic growth (Nozaka 2005; Plümper et al. 2012). Since coarse clinopyroxene II and olivine II grains display textures similar to bastite and/or mesh textures occurring in serpentinites, we suggest that they crystallized from pseudomorphic serpentine. Presence of minute magnetite inclusions in these grains also confirms their development from former serpentine phases, because magnetite, together with lizardite, is a commonly crystallizing phase during low-T serpentinization (Evans 2010). Clinopyroxene II and olivine II inherited probably serpentine textures and/or magnetite inclusions during deserpentinization, a process in which serpentine is dehydrated due to increased temperature and/or pressure (Plümper et al. 2012; Debret et al. 2013).

Occurrence of olivine II solely as intergrowths with serpentine suggests that deserpentinization was probably a short process. Mineral succession in the BBM serpentinites involving pseudomorphic lizardite/chrysotile, non-pseudomorphic antigorite and secondary olivine and clinopyroxene corresponds probably to three steps of alteration, typical of prograde metamorphism: (1) low-T serpentinization, (2) high-T recrystallization and (3) deserpentinization.

Such a style of alteration occurs typically in orogenic serpentinites. For example, serpentinites from the Lanzo Massif in Western Alps contain similar mineral succession represented by lizardite – antigorite – secondary olivine associated with chlorite or secondary clinopyroxene, amphibole and chlorite (Debret et al. 2013). Serpentinites from the Ladakh Massif in Himalayas consist mainly of antigorite replaced by secondary olivine containing magnetite and antigorite inclusions (Hattori

and Guillot 2007). However, in contrast to Lanzo and Ladakh massifs, mafic and ultramafic rocks from the BBM do not contain any minerals indicative of high-pressure conditions. At low-pressure conditions, formation of secondary olivine is expected at 380 °C, whereas secondary clinopyroxene appears at 450 °C in the system CaO–MgO–SiO_2–H_2O (Fig. 13, Nozaka 2005; Andreani et al. 2007; Plümper et al. 2012 and references therein). If true, this confirms general low-grade metamorphic conditions for the BBM serpentinites, similarly to lithologies from other Central-Sudetic Ophiolites (Kryza and Pin 2010).

7. Conclusions

Relationships between serpentinites and gabbros occurring in the Braszowice–Brzeźnica Massif suggest that serpentinites were intruded by gabbroic melts which either formed veins or crystallized in larger bodies. Occurrence of chromitites and melt-impregnation phases typically marks the transition from peridotite to gabbro in the oceanic lithosphere. The contact between serpentinites and gabbros is very poorly exposed, and thus it can only be speculated that it represented the paleo-Moho. The serpentinites contain small volume of non-serpentine phases: olivine, clinopyroxene, spinel and tremolite. Clinopyroxene and spinel originated due to MORB-like melt percolation. Composition of spinel suggests the back-arc setting of the Braszowice–Brzeźnica Massif, similarly to the previously studied chromite from the associated chromitites. Part of olivine originated during deserpentinization which affected all exposed serpentinites. The metamorphic event is also suggested by very low concentrations many of the fluid-mobile elements (Cs, Rb, Th, U, Pb and As), except Ba and Sr, which are enriched. In the eastern BBM, tremolite marks the contact metamorphism by the neighbouring granitic intrusion.

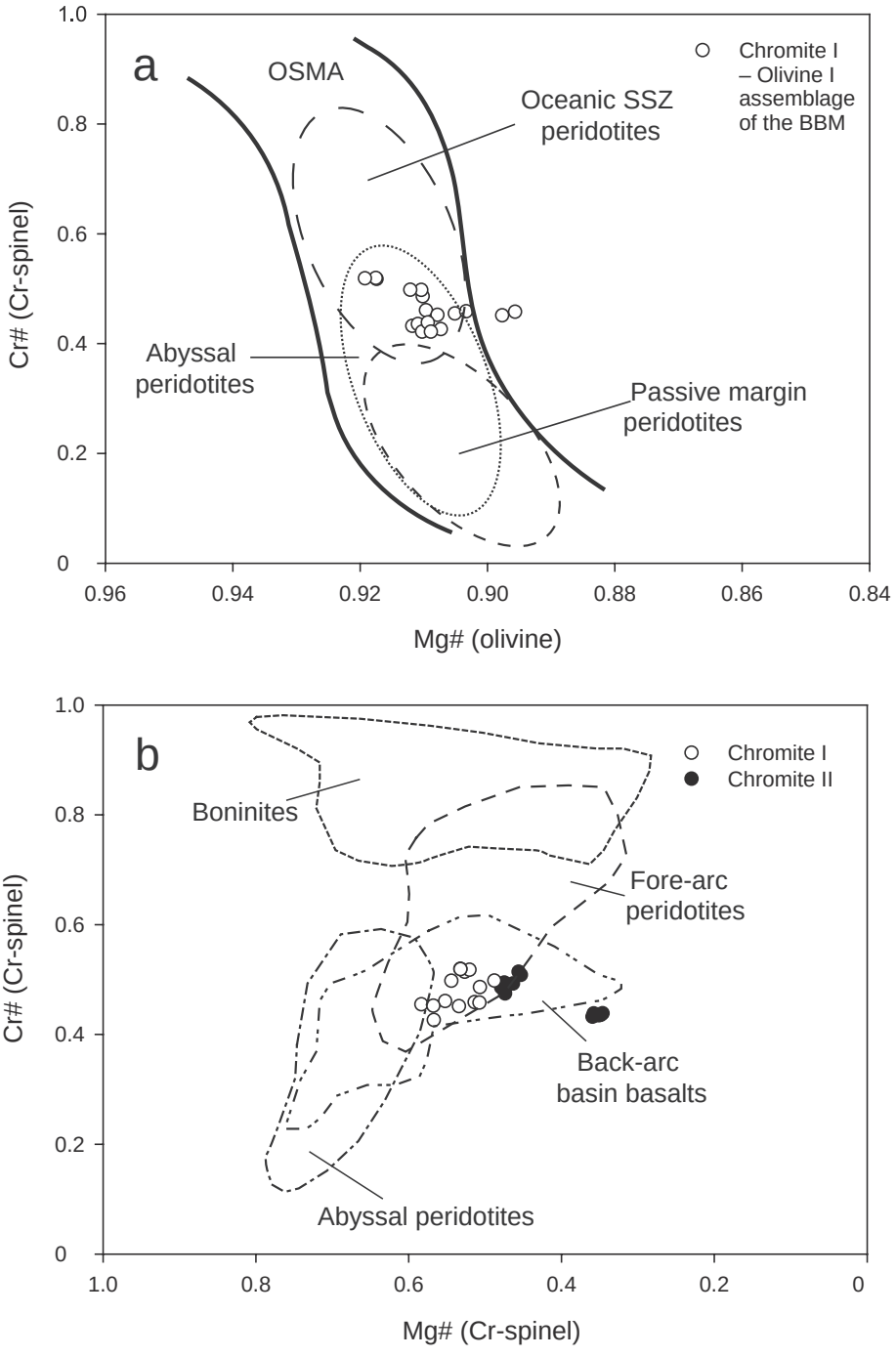

Fig. 12a – Spinel Cr# versus olivine Mg# plot for the assemblage olivine I–chromite I in the OSMA (olivine–spinel mantle array; Arai, 1994). The fields of abyssal peridotites, oceanic supra-subduction zone (SSZ) and passive-margin peridotites after Kaczmarek et al. (2015 and references therein) . **b** – Relationships between Cr# and Mg# in chromites from serpentinites from the western part of the Braszowice–Brzeźnica Massif. The fields of abyssal peridotites, fore-arc peridotites, back-arc basin basalts and boninites after the compilation of Kaczmarek et al. (2015 and references therein)

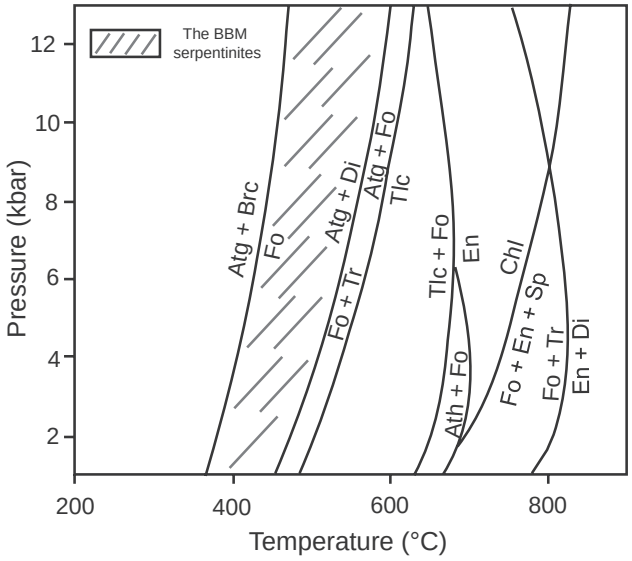

Fig. 13 Pressure–temperature diagram showing the metamorphic conditions of deserpentinization phases from the BBM, on the basis of equilibria in the CMASH ultrabasic system after Nozaka (2005).

The Braszowice–Brzeźnica and the Gogołów–Jordanów serpentinite massifs in Central Sudetes display several features in common: predominance of non-pseudomorphic antigorite serpentinites, occurrence of chemically and texturally similar chromitite bodies, evidence for melt percolation and presence of deserpentinization phases. This suggests that both these serpentinite complexes shared a similar geological history.

Acknowledgements. This paper was prepared as a part of the project of the National Science Centre of Poland ("Evolution of the serpentinitic members of ophiolites from Lower Silesia", DEC-2012/07/N/ST10/03934). Comments on the manuscript by two anonymous reviewers helped us to improve the manuscript. The authors are grateful to handling editor E. Jelínek for his helpful remarks. Comments and language correction of V. Janoušek significantly improved this paper. Thanks go to K. Dymna, P. Matz (University of Wrocław), F. Kiraly (University of Vienna) and M. Bukała (AGH University of Science and Technology) for their technical and analytical assistance.

References

Andreani M, Mevel C, Boullier AM, Escartin J (2007) Dynamic control on serpentine crystallization in veins: constraints on hydration processes in oceanic peridotites. Geochem Geophys Geosyst 8: doi: 10.1029/2006GC001373

Arai S (1994) Characterization of spinel peridotites by olivine–spinel compositional relationships: review and interpretation. Chem Geol 113: 191–204

Bédard JH (1999) Petrogenesis of boninites from the Betts Cove Ophiolite, Newfoundland, Canada: identification of subducted source components. J Petrol 40: 1853–1889

Bodinier J-L (1988) Geochemistry and petrogenesis of the Lanzo peridotite body, Western Alps. Tectonophysics 149: 67–88

Brunelli D, Cipriani A, Ottolini L, Peyve A, Bonatti E (2003) Mantle peridotites from the Bouvet Triple Junction Region, South Atlantic. Terra Nova 15: 194–203

Brunelli D, Seyler M, Cipriani A, Ottolini L, Bonatti E (2006) Discontinuous melt extraction and weak refertilization of mantle peridotites at the Vema lithospheric section (Mid-Atlantic Ridge). J Petrol 47: 745–771

Coogan LA, Kempton PD, Saunders AD, Norry MJ (2000) Melt aggregation within the crust beneath the Mid-Atlantic Ridge: evidence from plagioclase and clinopyroxene major and trace element compositions. Earth Planet Sci Lett 176: 245–257

Debret B, Nicollet C, Schwartz S, Andreani M, Godard M (2013) Three steps of serpentinization in an eclogitized oceanic serpentinization front (Lanzo Massif – Western Alps). J Metamorph Geol 31: 165–186

Delura K (2012) Chromitites from the Sudetic Ophiolite: Origin and Alteration. Archivum Mineralogiae Monographs 4, pp 1–91

Deschamps F, Godard M, Guillot S, Hattori K (2013) Geochemistry of subduction zone serpentinites: a review. Lithos 178: 96–127

Dubińska E, Gunia P (1997) The Sudetic Ophiolite: current view on its geodynamic model. Geol Q 41: 1–20

Dubińska E, Bylina P, Kozłowski A, Dőrr W, Nejbert K (2004) U–Pb dating of serpentinization: hydrothermal zircon from a metasomatic rodingite shell (Sudetic Ophiolite, SW Poland). Chem Geol 203: 183–203

Dziedzic H (1989) Tectonics and petrogenesis of Braszowice gabbro. In: Narębski W, Majerowicz A (eds) Lower and Upper Paleozoic Metabasites and Ophiolites of the Polish Sudetes. Excursion Guide. Wydawnictwo Uniwersytetu Wrocławskiego, Wrocław, pp 124–156 (in Polish)

Dziedzic H (1995) Pressure and temperature conditions of the Braszowice gabbro crystallization, Sudetic Foreblock. Geol Sudetica 29: 105–129 (in Polish)

Dziedzic K, Dziedzic H (2000) Genetic relationship between metabasalts and related gabbroic rocks: an example from the Fore-Sudetic Block, SW Poland. Geol Sudetica 33: 33–48

Evans BW (2010) Lizardite versus antigorite serpentinite: magnetite, hydrogen and life (?). Geology 38: 879–882

Finckh L (1929) Geologische Karte von Preussen und benachbarten deutschen Ländern, Blatt Frankenstein 1 : 25 000. Preussisches Geologisches Landesamt, Berlin (in German)

Franke W, Dulce J-W (2017) Back to sender: tectonic accretion and recycling of Baltica-derived Devonian clastic

sediments in the Rheno-Hercynian Variscides. Int J Earth Sci 106: 377–386

Frost BR (1975) Contact metamorphism of serpentinite, chloritic blackwall and rodingite at Paddy-Go-Easy Pass, Central Cascades, Washington. J Petrol 16: 272–313

Gaździk J (1957) Geological map of Sudetes 1:25000, sheet Przyłęk. Państwowy Instytut Geologiczny, Warszawa (in Polish)

Godard M, Jousselin D, Bodinier J-L (2000) Relationships between geochemistry and structure beneath a palaeo-spreading centre: a study of the mantle section in the Oman Ophiolite. Earth Planet Sci Lett 180: 133–148

Gunia P (1992) Petrology of the ultrabasic rocks from Braszowice–Brzeźnica Massif (Fore-Sudetic Block). Geol Sudetica 26: 119–170

Hattori KH, Guillot S (2007) Geochemical character of serpentinites associated with high- to ultrahigh-pressure metamorphic rocks in the Alps, Cuba and the Himalayas: recycling of elements in subduction zones. Geochem Geophys Geosyst 8: doi: 10.1029/2007GC001594

Jašarová P, Racek M, Jeřábek P, Holub F (2016) Metamorphic reactions and textural changes in coronitic metagabbros from the Teplá Crystalline and Mariánské Lázně complexes, Bohemian Massif. J Geosci 61: 193–219

Jelínek E, Štědrá V, Cháb J (1997) The Mariánské Lázně Complex. In: Vrána S, Štědrá V (eds) Geological Model of Western Bohemia Related to the KTB Borehole in Germany. Sbor Geol Věd, Geol 47: 61–70

Jochum KP, Weis U, Stoll B, Kuzmin D, Yang Q, Raczek I, Jacob DE, Stracke A, Birbaum K, Frick DA, Günther D, Enzweiler J (2011) Determination of reference values for NIST SRM 610–617 glasses following ISO guidelines. Geost Geoanal Res 35: 397–429

Kaczmarek MA, Jonda L, Davies HL (2015) Evidence of melting, melt percolation and deformation in a suprasubduction zone (Marum Ophiolite Complex, Papua New Guinea). Contrib Mineral Petrol 170: doi: 10.1007/s00410-015-1174-z

Kodolanyi J, Pettke T (2011) Loss of trace elements from serpentinites during fluid-assisted transformation of chrysotile to antigorite – an example from Guatemala. Chem Geol 284(3–4): 351–362

Koga KT, Kelemen PB, Shimizu N (2001) Petrogenesis of the crust–mantle transition zone and the origin of lower crustal wehrlite in the Oman Ophiolite. Geochem Geophys Geosyst 2: doi: 10.1029/2000GC000132

Kretz R (1983) Symbols for rock-forming minerals. Amer Miner 68: 277–279

Kryza R, Pin C (2010) The Central-Sudetic ophiolites (SW Poland): petrogenetic issues, geochronology and palaeotectonic implications. Gondwana Res 17: 292–305

Mazur S, Turniak K, Szczepański J, McNaughton NJ (2015) Vestiges of Saxothuringian crust in the Central Sudetes, Bohemian Massif: zircon evidence of a recycled subducted slab provenance. Gondwana Res 27: 825–839

McDonough WF, Sun SS (1995) The composition of the Earth. Chem Geol 120: 223–253

Morimoto N, Fabries J, Ferguson AK, Ginzburg IV, Ross M, Seifert FA, Zussman J, Aoki K, Gottardi G (1988) Nomenclature of pyroxenes. Amer Miner 73: 1123–1133

Morishita T, Tani K, Shukuno H, Harigane Y, Tamura A, Kumagai H, Hellebrand E (2011) Diversity of melt conduits in the Izu–Bonin–Mariana forearc mantle: implications for the earliest stage of arc magmatism. Geology 39: 411–414

Murphy JB, Gutiérrez-Alonso G, Nance RD, Fernández-Suárez J, Keppie JD, Quesada C, Strachan RA, Dostal J (2006) Origin of the Rheic Ocean: rifting along a Neoproterozoic suture? Geology 34: 325–328

Nance RD, Linnemann U (2009) The Rheic Ocean: origin, evolution and significance. GSA Today 18: 4–12

Nance RD, Gutiérrez-Alonso G, Keppie JD, Linnemann U, Murphy JB, Quesada C, Strachan RA, Woodcock NH (2010) Evolution of the Rheic Ocean. Gondwana Res 17: 194–222

Nozaka T (2005) Metamorphic history of serpentinite mylonites from the Happo ultramafic complex, central Japan. J Metamorph Geol 23: 711–723

Nozaka T, Shibata T (1995) Mineral paragenesis in thermally metamorphosed serpentinites, Ohsa-yama, Okayama Prefecture. Okayama Univ Earth Sci Rep 2: 1–12

Oberc J, Badura J, Przybylski B (1996) Geological map of Sudetes 1:25000, sheet Bardo Śląskie. Państwowy Instytut Geologiczny, Warszawa (in Polish)

Ohara Y, Stern RJ, Ishii T, Yurimoto H, Yamazaki T (2002) Peridotites from the Mariana Trough: first look at the mantle beneath an active back-arc basin. Contrib Mineral Petrol 143: 1–18

Oliver GJH, Corfu F, Krogh TE (1993) U–Pb ages from SW Poland: evidence for a Caledonian suture zone between Baltica and Gondwana. J Geol Soc, London 150: 355–369

Pearce JA, Barker PF, Edwards SJ, Parkinson IJ, Leat PT (2000) Geochemistry and tectonic significance of peridotites from the South Sandwich arc–basin system, South Atlantic. Contrib Mineral Petrol 139: 36–53

Pin C, Majerowicz A, Wojciechowska I (1988) Upper Paleozoic oceanic crust in the Polish Sudetes: Nd–Sr isotope and trace element evidence. Lithos 21: 195–209

Plümper O, Piazolo S, Austrheim H (2012) Olivine pseudomorphs after serpentinized orthopyroxene record transient oceanic lithospheric mantle dehydration (Leka Ophiolite Complex, Norway). J Petrol 53: 1–26

Pouchou JL, Pichoir J (1984) A new model for quantitative X-ray microanalysis. Le Rech Aerospat 3: 167–192

Seyler M, Cannat M, Mével C (2003) Evidence for major element heterogeneity in the mantle source of

abyssal peridotites from the Southwest Indian Ridge (52 to 68°E). Geochem Geophys Geosyst 4: doi: 10.1029/2002GC000305

Seyler M, Lorand JP, Dick HJB, Drouin M (2007) Pervasive melt percolation reactions in ultra-depleted refractory harzburgites at the Mid Atlantic Ridge, 15°20'N: ODP Hole 1274A. Contrib Mineral Petrol 153: 303–319

Suhr G, Kelemen P, Paulick H (2008) Microtextures in Hole 1274A peridotites, ODP Leg 209, Mid-Atlantic Ridge: tracking the fate of melts percolating in peridotite as the lithosphere is intercepted. Geochem Geophys Geosyst 9: doi: 10.1029/2007GC001726

Sun SS, McDonough WF (1989) Chemical and isotopic systematics of oceanic basalts: implications for mantle composition and processes. In: Saunders AD, Norry MJ (eds) Magmatism in the Ocean Basins. Geological Society, London, Special Publications 42, pp 313–345

Tamura A, Arai S (2006) Harzburgite–dunite–orthopyroxenite suite as a record of supra subduction zone setting for the Oman Ophiolite mantle. Lithos 90: 43–56

Trommsdorff V, Evans BW (1972) Progressive metamorphism of antigorite schist in the Bergell tonalite aureole (Italy). Amer J Sci 272: 423–437

Trommsdorff V, Connolly JAD (1996) The ultramafic contact aureole about the Bregaglia (Bergell) tonalite: isograds and a thermal model. Schweiz Mineral Petrogr Mitt 76: 537–547

Trommsdorff V, Evans BW (1977) Antigorite-ophicarbonates: contact metamorphism in Valmalenco, Italy. Contrib Mineral Petrol 62: 301–312

van Achterbergh E, Ryan CG, Jackson SE, Griffin WL (2001) Data reduction software for LA-ICP-MS. In: Sylvester PJ (ed) Laser-Ablation-ICPMS in the Earth Sciences: Principles and Applications. Mineralogical Association of Canada, Short Course Series 29: pp 239–243

Wicks FJ, Whittaker EJW (1977) Serpentine textures and serpentinization. Canad Mineral 15: 459–488

Wojtulek PM, Puziewicz J, Ntaflos T, Bukała M (2016a) Podiform chromitites from the Variscan ophiolite serpentinites of Lower Silesia (SW Poland) – petrologic and tectonic setting implications. Geol Q 60: 56–66

Wojtulek PM, Puziewicz J, Ntaflos T (2016b) Melt impregnation phases in the mantle section of the Ślęża Ophiolite (SW Poland). Chem Erde 76: 299–308